Design and Development of Electrospun Membranes Loaded with Novel Nanoparticles for Wound Healing

MS Thesis

By

Hafsa Azhar

CIIT/FA21-R06-026/LHR

COMSATS University Islamabad

Lahore Campus – Pakistan

Spring 2023

Design and Development of Electrospun Membranes Loaded with Novel Nanoparticles for Wound Healing

A Thesis submitted to
COMSATS University Islamabad, Lahore Campus

In partial fulfillment
of the requirement for the degree of

Master of Science
in
Chemistry

by

Hafsa Azhar

CIIT/FA21-R06-026/LHR

COMSATS University Islamabad
Lahore Campus – Pakistan

Spring 2023

Design and Development of Electrospun Membrane Loaded with Novel Nanoparticles for Wound Healing

This Thesis is submitted to the Department of Chemistry as partial fulfillment of the requirements for the award of a degree of MS in Chemistry.

Name	Registration Number
Hafsa Azhar	**CIIT/FA21-R06-026/LHR**

Supervisor

Prof. Dr. Anila Asif

Professor

Interdisciplinary Research Centre in Biomedical Materials (IRCBM)

Lahore Campus

COMSATS University Islamabad (CUI) Lahore Campus.

June 2023

Co-Supervisor

Dr. Arsalan Ahmed

Assistant Professor

Interdisciplinary Research Centre in Biomedical Materials (IRCBM)

Lahore Campus

COMSATS University Islamabad (CUI) Lahore Campus.

June 2023

Certificate of Approval

This thesis titled

Design and Development of Electrospun Membranes Loaded with Novel Nanoparticles for Wound Healing

By

Hafsa Azhar

CIIT/FA21-R06-026/LHR

Has been approved

For the COMSATS University Islamabad, Lahore Campus

External Examiner: …….

Name

University address

Supervisor: ……..

Prof. Dr. Anila Asif

COMSATS University Islamabad, Lahore Campus

Co-supervisor: …….

Dr. Arsalan Ahmed

COMSATS University Islamabad, Lahore Campus

HoD: ……

Prof. Dr. Zulfiqar Ali

Department of Chemistry, COMSATS University Islamabad, Lahore Campus

Declaration

I, Hafsa Azhar, CIIT/FA21-R06-023/LHR hereby declare that I have produced the work presented in this thesis, during the scheduled period of study. I also declare that I have not taken any material from any source except referred to wherever due that amount of plagiarism is within an acceptable range. If a violation of HEC rules on research has occurred in this thesis, I shall be liable to punishable action under the plagiarism rules of the HEC.

Date: _____

_____

Hafsa Azhar

CIIT/FA21-R06-026/LHR

Certificate

It is certified that Hafsa Azhar, CIIT/FA21-R06-023/LHR has carried out all the work related to this thesis under my supervision at IRCBM, COMSATS University Islamabad, Lahore Campus, and the work fulfills the requirement for the award of MS degree.

Date: _____

Supervisor:
Prof. Dr. Anila Asif
Professor

Interdisciplinary Research Centre in Biomedical Materials (IRCBM)

COMSATS University Islamabad, Lahore Campus

Dedication

I would like to dedicate this thesis to my parents and siblings who have always loved me and taught me to work hard for all the challenges that I aspire to achieve. And to my respected supervisor Prof. Dr. Anila Asif who has been a constant source of knowledge, strength, and encouragement throughout my entire journey.

Acknowledgments

In the name of Allah, the Most Gracious, the Most Merciful.

I begin this acknowledgment by expressing my deep gratitude to Allah Almighty, the source of all knowledge, wisdom, and guidance. His blessings and mercy have been instrumental in every step of this thesis journey. Grateful to the Head of the Chemistry department **Prof. Dr. Zulfiqar Ali** and the whole chemistry department for an opportunity and support for research. I would like to thank the Head of IRCBM **Prof. Dr. Aqif Anwar Chaudhary** for providing a great opportunity of research at IRCBM. I would like to extend my heartfelt appreciation to my supervisor, **Prof. Dr. Anila Asif,** for her unwavering support, guidance, and expertise throughout this research. Her invaluable feedback, constructive criticism, and continuous encouragement have played a crucial role in shaping the direction and quality of this thesis. I am truly grateful for her mentorship and the opportunities she provided me to grow academically. I would also like to thank my co-supervisor **Dr. Arsalan Ahmed** as well as **Dr. Hamad Khalid** for their valuable insights, suggestions, and scholarly contributions. I am indebted to them for their time and patience. I would also like to acknowledge the support and encouragement of the ***faculty members*** and ***supporting staff*** at IRCBM. Furthermore, I would like to express my deep appreciation to my friends and colleagues, ***Hina Khadim*** and ***Mehreen Zahra*****.** Their support, encouragement, and intellectual discussions have been a constant source of inspiration and motivation for me. Finally, I express my heartfelt gratitude to my **family** for their unconditional love, firm support, and endless prayers. Their belief in me and their sacrifices have been the key to my success. I am forever grateful for their encouragement and understanding. To everyone mentioned above and all those who have supported me in any way but could not be named here, I extend my sincere appreciation. Your contributions, whether big or small, have shaped this thesis and my academic growth, and I am truly grateful. All praise and thanks to Allah. Alhamdulillah.

Hafsa Azhar

CIIT/FA21-R06-026/LHR

Abstract

Design and Development of Electrospun Membranes Loaded with Novel Nanoparticles for Wound Healing

By

Hafsa Azhar

This research study investigated the design and development of electrospun membranes loaded with novel nanoparticles for wound healing. The primary focus of this work was to address the challenges associated with wound dressings, with the need for enhanced wound healing, optimization of electrospun membranes, and sustained release of drugs. To achieve these goals, electrospun membranes composed of polymers such as cellulose acetate, polyurethane (PU), and polyvinyl alcohol (PVA) were fabricated. Nanoparticles of ciprofloxacin were incorporated into the electrospun membranes to impart additional functionalities and promote wound healing. The methodology employed two key techniques: electrospinning and the ion gelation method. Electrospinning was used to fabricate the membranes, providing control over key properties such as pore size, mechanical strength, porosity, and morphology. The ion gelation method was utilized for the synthesis of chitosan-ciprofloxacin nanoparticles, which were subsequently loaded into the electrospun membranes. The comparison of sheets with free ciprofloxacin and nanoparticles of ciprofloxacin was carried out in this study. Characterizations of the membranes and nanoparticles were performed using FESEM, FTIR, XRD, TGA, density measurements, contact angle measurements, antibacterial studies and drug release. These analyses allowed for the assessment of morphology, chemical composition, crystallinity, thermal stability, and surface wettability of the materials.

Table Of Contents

List of Figures

List of Tables

Chapter 1

Introduction

1.1 Tissue Regeneration

Tissue regeneration is a multidisciplinary field that combines engineering and biological principles to create replacements for diseased or damaged tissues. It has emerged as a promising method for repairing or replacing damaged tissues and organs. Tissue engineering has made significant progress in recent years, with an increasing number of tissue constructs being produced for various medical applications [1]. However, many challenges remain to be overcome in order to bring tissue engineering closer to clinical translation. By combining biomaterials, cells, and biologically active molecules, this field aims to create functional tissues and organs. One of the most promising applications of tissue engineering is in the field of wound healing, where it can help with tissue regeneration and wound healing [2].

There are two types of tissue engineering approaches for wound healing: cellular and acellular. Cellular approaches involve the use of cells to regenerate damaged tissue, such as stem cells or skin cells. Acellular approaches, on the other hand, use biomaterials and growth factors to aid wound healing in the absence of cells [3].

Different cell types are used in cellular approaches to tissue engineering for wound healing. These cells can be harvested from the patient's own tissue or from a donor and cultured in the laboratory before being implanted into the wound site. The cells can then differentiate into the various cell types required for wound healing, such as fibroblasts, endothelial cells, and epithelial cells. Cellular approaches have the advantage of potentially providing more complete and natural wound tissue regeneration, but they can be difficult due to the need to isolate and culture the cells [4].

Different cell types are used in cellular approaches to tissue engineering for wound healing. These cells can be harvested from the patient's own tissue or from a donor and cultured in the laboratory before being implanted into the wound site. The cells can then

differentiate into the various cell types required for wound healing, such as fibroblasts, endothelial cells, and epithelial cells. Cellular approaches have the advantage of potentially providing more complete and natural wound tissue regeneration, but they can be difficult due to the need to isolate and culture the cells [4].

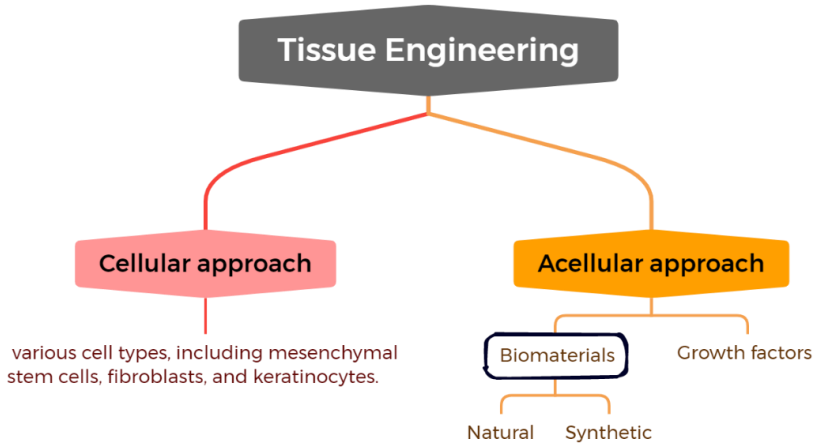

Figure 1.1 Categories of tissue engineering approaches

Skin tissue engineering is now regarded as a viable and efficient method for restoring fully functional tissue through the use of new biomaterials or custom-made scaffold [5]. The scaffolds can cover wounds, act as a temporary barrier against external infections, and guide the rearrangement of skin cells while promoting host tissue integration. To encourage cell attachment, multiplication, and differentiation, the ideal tissue engineering scaffold must have appropriate surface microstructures and biochemistry, as well as sufficient physical and mechanical strength.

1.2 Biomaterials

Biomaterials are materials that can interact with living tissues without causing harm to biological systems. They can be synthetic or natural in origin, and their properties can be tailored to match those of the tissue's native ECM. The ECM is a complex web of proteins and other substances that supports the structural integrity of cells and regulates their behavior [6].

Biomaterials are critical in tissue engineering because they provide an infrastructure for cells to adhere, multiply, and differentiate into the desired tissue type. They play an important role in wound healing by providing a supportive environment for the body's natural healing processes [7]. The use of biomaterials in tissue regeneration approaches to wound healing has demonstrated great promise in terms of promoting new tissue formation and enhancing the healing process. Several biomaterials, including natural and synthetic polymers, as well as composite materials, have been investigated for their potential use in tissue engineering. The biomaterials used in a tissue engineering application are chosen based on the type of tissue being regenerated, the intended function of the tissue, and the mechanical and biological requirements of the tissue construct [8].

1.2.1 Properties of biomaterials

To encourage cell fixation, proliferation, and differentiation, biomaterials used in tissue engineering should have unique properties such as biocompatibility, biodegradability, toughness, porosity, and antibacterial properties [9]. Depending on the application, the properties of biomaterials used in wound healing can vary. When in contact with living tissue, the biomaterial should not elicit an adverse immune response [10]. *Biodegradable:* It should degrade over time as new tissue forms, allowing for complete wound healing. [11]. *Porous:* It should have a pore of sufficient size to allow for cell invasion and the nutrients required for tissue regeneration. *Mechanical strength:* The biomaterial should be strong enough to withstand the mechanical stresses of the wound site, yet flexible enough to conform to the wound bed. [12]. *Antibacterial properties:* It should be capable of inhibiting bacterial growth and lowering the risk of infection. [11].

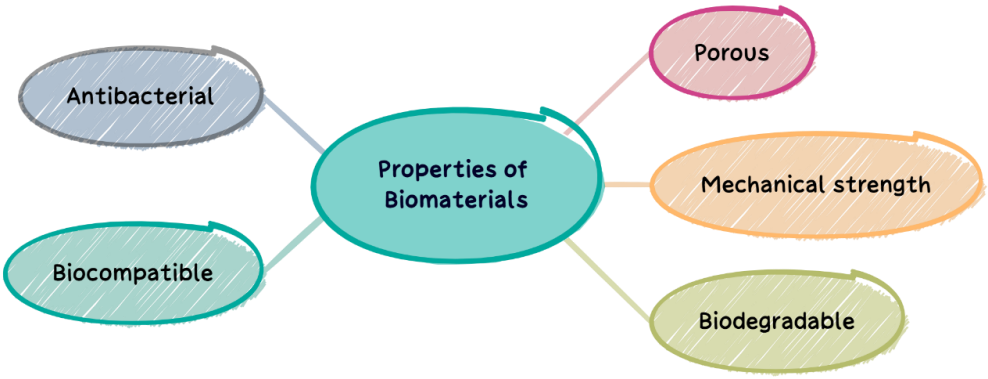

Figure 1.2 Properties required in biomaterials for tissue engineering

1.2.2 Methods of fabricating wound dressings

Wound dressings are a common way for biomaterials to be delivered to the wound site. They can prevent further damage to the wound, provide a moist environment for healing, and deliver therapeutic agents to promote wound healing. Wound dressings can be made using a variety of techniques, including:

1.2.2.1 Electrospinning:

Electrospinning is the process of creating nanofiber mats by applying an electric field to a polymer solution or melt. Because of the electric field, the polymer solution stretches and forms a thin fibre, which is then collected onto a collector to form a mat. Electrospun nanofiber mats have an excellent surface area-to-volume ratio, making them ideal for wound dressing. They can be combined with therapeutic agents like growth factors and antibiotics to improve wound healing. [13].

1.2.2.2 Freeze-drying:

Freeze-drying is a method of producing porous biomaterials that involves freezing a solution or suspension of the material and then removing the water through sublimation under a vacuum. The high surface area and interconnected porosity of freeze-dried biomaterials allow for high drug loading and controlled drug release. By incorporating

therapeutic agents such as growth factors and antimicrobials into the material, freeze-dried biomaterials can be used as wound dressings. [14].

1.2.2.3 Solvent casting:

Solvent casting is a method of creating biomaterial films that involves dissolving the material in a solvent and then casting the solution onto a surface to form a film. Solvent casting can be used to create biomaterial films with a variety of properties, including thickness, mechanical strength, and drug release. To improve their antimicrobial and anti-inflammatory properties, the films can be functionalized with therapeutic agents such as silver nanoparticles and curcumin. [15].

1.2.2.4 Spraying:

Spraying is a method of applying biomaterial coatings to the wound surface with a spray gun. To improve wound healing, the biomaterial can be in the form of a solution or suspension, and it can be functionalized with therapeutic agents such as growth factors and antimicrobials. Spraying allows for precise control of coating thickness and therapeutic agent delivery to the wound site. [16].

1.2.2.5 Hydrogel formation:

Hydrogel formation is a method of creating biomaterials capable of absorbing large amounts of water and forming a gel-like structure. Hydrogels can be used as wound dressings because they can keep wounds moist and release therapeutic agents over time. To improve wound healing, hydrogels can be functionalized with therapeutic agents such as growth factors and antibiotics. [17].

1.2.3 Electrospinning

Electrospinning is a method for creating nanofibers with diameters ranging from a few nanometres to several micrometres. These fibres can be made from a variety of materials, including natural and synthetic polymers, and used for a variety of purposes, including wound healing. [18].

A syringe pump, a high-voltage supply, a nozzle, and a grounded collector are typical electrospinning components. The polymer solution is injected into the syringe, and the spinneret is moved away from the collector. When the power supply is activated, an electrical potential is applied between the spinneret and the rotating drum. As a result, a Taylor cone forms at the spinneret's tip, and a fine stream of polymer solution is ejected from it. The jet of polymer solution travels towards the grounded collector, undergoing stretching and whipping as a result of the electrostatic forces acting on it. As a result, nanofibers are formed and collected on the collector. [19].

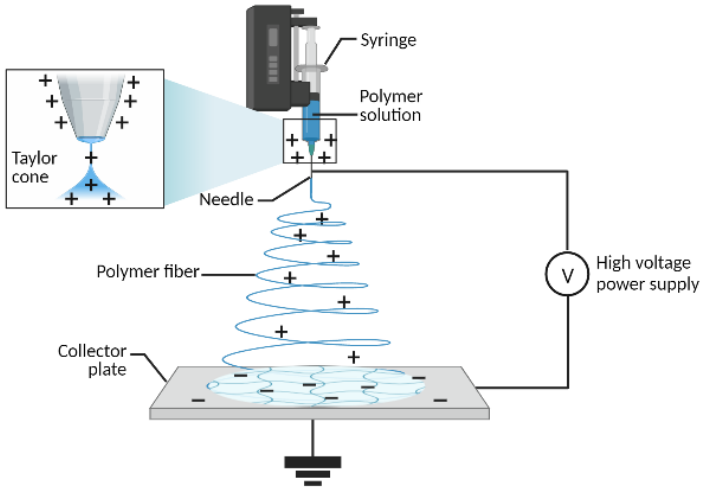

Figure 1.3 Electrospinning setup

The electrospinning technique's ability to produce ultra-fine polymer fibres has made it a popular choice in the biomedical field. The resulting electrospun fibres have outstanding properties such as high porosity, a large surface area, and durability. Furthermore, an electrospinning machine can easily process a wide range of biomaterials, including bio-ceramics and metals.[20].

The structural similarity of these micro/nano electrospun fibres to the extracellular matrix of the skin improves their cell differentiation, adhesion, migration, and proliferation properties. As a result, they are a good material for wound dressings because they allow for the controlled release of bio factors like nanoparticles, genes, and proteins, as well as the continuous diffusion of oxygen and nutrients.[21].

Flow rate, polymer concentration, and electric field strength can all be adjusted to control the morphology of the fibres. Because of these advantages, electrospun fibres are a promising candidate for use in tissue regeneration and drug delivery.

1.2.3.1 Polymers and their significance

Wound dressings can be made from both synthetic and organic polymers. However, natural biopolymers are more attractive for this purpose owing to their suitability for biological use, degradability, extensive biomimicry, and good physicochemical properties. These qualities make natural biopolymers structurally similar to the extracellular matrix (ECM) and therefore ideal for wound dressings [22].

1.2.3.1.1 Cellulose acetate (CA)

Cellulose acetate is a thermoplastic polymer that is produced by chemically modifying cellulose, a naturally occurring polysaccharide found in plant cell walls. As part of the modification process, cellulose is reacted with acetic acid, acetic anhydride, and sulfuric acid in the presence of a catalyst. The resulting cellulose acetate is a white, odorless, and tasteless solid material that is solvable in acetone, dimethylacetamide, ethyl acetate, and chloroform. The level of substitution, or the quantity of acetyl groups attached to the cellulose molecules, determines the solubility and other properties of cellulose acetate.

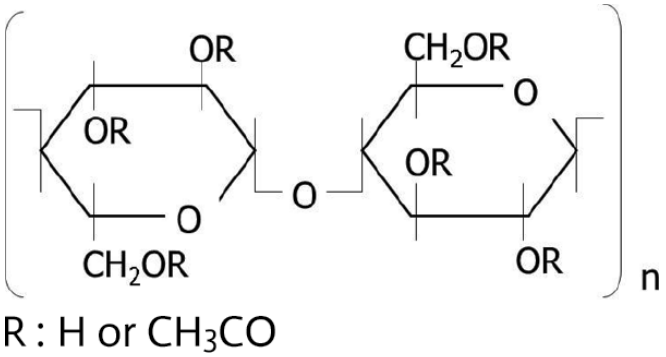

Figure 1.4 Structure of cellulose acetate (CA)

Cellulose acetate (CA) is biocompatible, biodegradable, and non-toxic material, relatively low cost, and has excellent resistance to heat and chemicals. Cellulose triacetate and diacetate are two types of cellulose derivatives, with the former being completely substituted and the latter partially substituted. Both types are typically dissolved in organic solvents rather than water.

CA has numerous potential industrial and biomedical applications, including tissue engineering, wound dressings, drug delivery systems, and antibacterial applications. [23]. CA nanofibers electrospun have proven particularly useful in biomedical applications. Electrospun CA nanofibers can be easily ejected from a syringe needle and deposited randomly on a collector due to their excellent electrical conductivity, allowing for controlled delivery of antioxidants, anti-inflammatory drugs, antibiotics, and vitamins. Overall, CA's properties make it a versatile and promising material for a wide range of biomedical applications.

It has been shown to promote wound healing by acting as a scaffold for the formation of new tissue and by increasing cellular proliferation and migration. CA has also shown a high level of hydrolytic stability and chemical resistance. Several studies have looked into the potential of cellulose acetate for wound healing.applications.

1.2.3.1.2 Polyvinyl alcohol (PVA)

Polyvinyl alcohol and other synthetic polymers have also been investigated for their potential in tissue engineering approaches to wound healing. PVA is a water-soluble synthetic polymer derived from the polymerization of vinyl acetate. PVA, a linear, semi-crystalline polymer, is produced by hydrolyzing vinyl acetate monomers in the presence of a catalyst. [24].

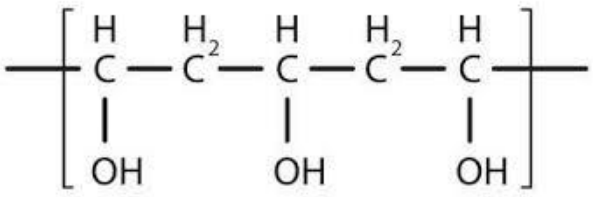

Figure 1.5 Structure of polyvinyl alcohol (PVA)

PVA has excellent film-forming and binding properties, which make it useful in a wide range of applications such as paper coatings, textiles, adhesives, and emulsions. It's also widely used in the manufacture of water-soluble packaging materials like laundry detergent pods and single-use plastics. PVA's biodegradability is one of its most significant advantages, making it a popular choice for environmentally friendly applications. When PVA is exposed to water, it gradually degrades into non-toxic monomers that can be safely released into the environment. Because of its biocompatibility, low toxicity, and water solubility, PVA has several potential biomedical applications in addition to its commercial applications. It can be used as a drug administration matrix, dressing materials, or tissue engineering scaffolds.

1.2.3.1.3 Polyurethane (PU)

Polyurethane is a type of polymer that is synthesized from the reaction of a polyol with diisocyanate. The basic reaction mechanism for the formation of polyurethane is as follows:

A polyol reacts with a diisocyanate. The polyol typically contains hydroxyl (-OH) groups, while the diisocyanate contains isocyanate (-NCO) groups. This reaction results in the formation of urethane (-NHCO-) linkages in the polymer chain.

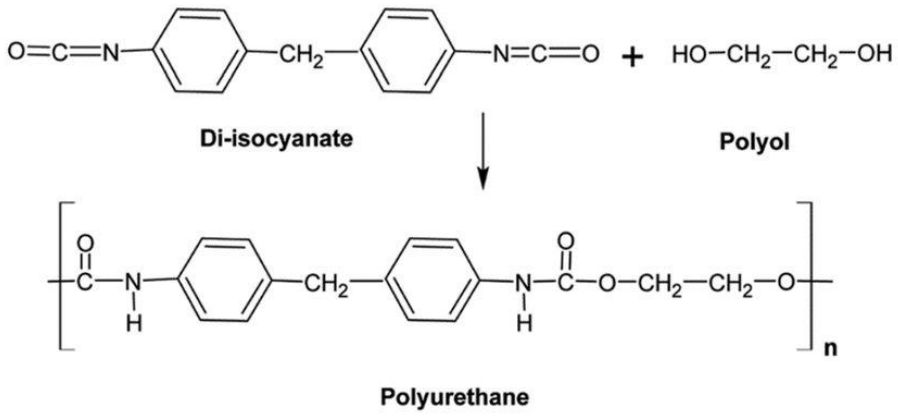

Figure 1.6 Formation of polyether polyurethane (PU)

Polyether polyurethane (PU) is a synthetic polymer that is used to make wound dressings. It is an elastomer that has long been used in both medical and non-medical applications.

Outstanding mechanical strength and hydrophobicity can be found in them. Polyurethane nanofibers are of great interest for utilization as wound care products in the medical industry, drug delivery, tissue regeneration, biosensor devices, cellular epithelization, stem cell differentiation, and the creation of protective clothing. It has been proved to promote wound healing by providing scaffold for the creation of new tissue and enhancing cellular proliferation and migration. Due to the distinctively porous character of the nanofibers, which only permits nutrient and gas passage, it acts as a barrier against microbial invasion.

Polyurethane's hydrophobic nature was a significant challenge as it hindered the exudate removal ability of wounds. However, this challenge has been overcome by incorporating cellulose acetate and polyvinyl alcohol into polyurethane fibers, which makes them hydrophilic to some extent, thus facilitating the healing process.

1.2.4 Application of biomaterials for wound healing

1.2.4.1 Wound

The wounds develop as a result of the skin tissue's integrity being compromised. A wound must be properly cared for, regardless of how slight or severe it is. Chronic wounds develop when microorganisms attack acute wounds. Wounds that do not heal are turning into a major problem on a global scale. Several wound dressings made from mixtures of non-natural or natural polymers have been created to help with the intricate process of wound healing. Although over 3,000 different wound dressings are on the market for different wounds, none can entirely heal them. It is difficult to create healing solutions for chronic wounds that are both efficient and affordable. Current research is focused on developing more efficient, affordable, biocompatible, and antimicrobial wound dressings for infectious wounds.

1.2.4.2 Types of wounds

Wounds can be categorized into two types: acute and chronic wounds. Acute wounds are those that heal within a specific time frame, usually less than six weeks. On the other hand, chronic wounds fail to heal within this time interval due to a variety of reasons such as bacterial infection, underlying diseases, or poor blood supply.

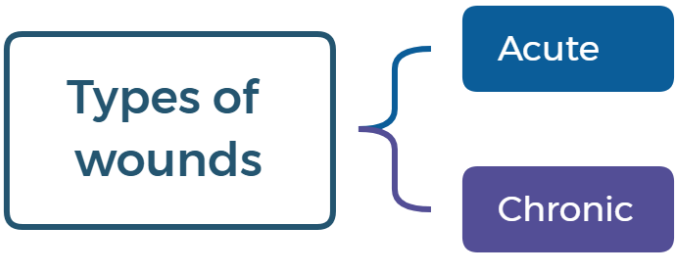

Figure 1.7 Types of wounds

1.2.4.2.1 Acute wounds

Acute wounds are those that go over the typical stages of wound recovery and restore the tissue in the best possible way. Irrespective of the sort of wound, it is termed acute while it occurs in its early stages. Acute injuries undergo a number of molecular mechanisms that eventually lead to structural integrity repair. The initial response to an acute wound is hemostasis, which stops bleeding and reduces blood loss. An injury to the skin causes an intricate immune response to be triggered during the inflammatory phase, which kills the pathogens entering the wound and gets the tissue ready for the recovery of anatomical integrity. In the latter, which takes place in the proliferative phase, granulation tissue is formed together with neovascularization and re-epithelialization [4,8]. The remodeling phase, which marks the end of acute wound healing, replaces the granulation tissue with a scar and clears the epidermis of immune cells that either die by apoptosis or move to the dermis.

1.2.4.2.2 Chronic wounds

If wounds are unable to go through the physiological process of wound healing, skin tissue repair is delayed, which eventually leads to chronic wounds. Exudation, recurrent infection, tissue necrosis, faulty re-epithelialization, reduced angiogenesis, and excessive ROS generation are typical characteristics of non-healing wounds. The three main kinds of chronic wounds are pressure ulcers, vascular sores, and diabetic foot ulcers (DFU). Typically, they are seen in senior adults with pathological illnesses such as diabetes, vascular disease, and obesity. They display a stage of continuous inflammation and microbial invasion, both of which lead to the formation of the biofilm.

We now understand a lot more about how both acute and chronic wounds heal microbial invasions in recent years. The unbalanced generation of growth factors, and inflammatory responses distinguish the healing of chronic wounds apart from that of acute wounds. Seventy percent of the most prevalent chronic wounds are venous pain and neuropathic ulcers.

1.2.4.3 Wound Repair

The complicated process of wound recovery necessitates the coordinated action of several cells, cytokines, and growth factors. In cases where the wound is deep or extensive, the body may not be able to heal the wound effectively, leading to chronic wounds that can be difficult to treat. Traditional wound treatments such as gauze dressings and topical medications may be insufficient for these types of wounds. In recent years, tissue engineering approaches for wound healing have shown great potential for promoting wound healing and regenerating damaged tissues.

1.2.4.3.1 Phases of wound repair

There are typically four phases of wound healing: hemostasis, inflammatory, proliferative, and maturation. Each phase involves a different set of cellular and molecular events that work together to repair and regenerate damaged tissue.

a) Hemostasis

The hemostasis phase is the initial response to tissue injury and occurs immediately after the wound is created. The goal of this phase is to stop bleeding and create a stable environment for wound healing. The blood vessels in the wound contract to reduce blood flow, and platelets aggregate to form a clot, which seals the wound and prevents further blood loss. The clot also releases growth factors and cytokines, which initiate the next phase of wound healing.

b) Inflammatory Phase:

The inflammatory phase begins within hours of the initial injury and lasts for up to 5 days. During this phase white blood cells are brought into the area of the wound to eradicate bacteria and debris, and to initiate the tissue repair process. Macrophages and neutrophils are two types of inflammatory cells that release cytokines and growth factors to stimulate the movement and proliferation of other cells involved in the healing procedure, such as fibroblasts and endothelial cells. The inflammatory phase is also characterized by redness, swelling, warmth, and pain.

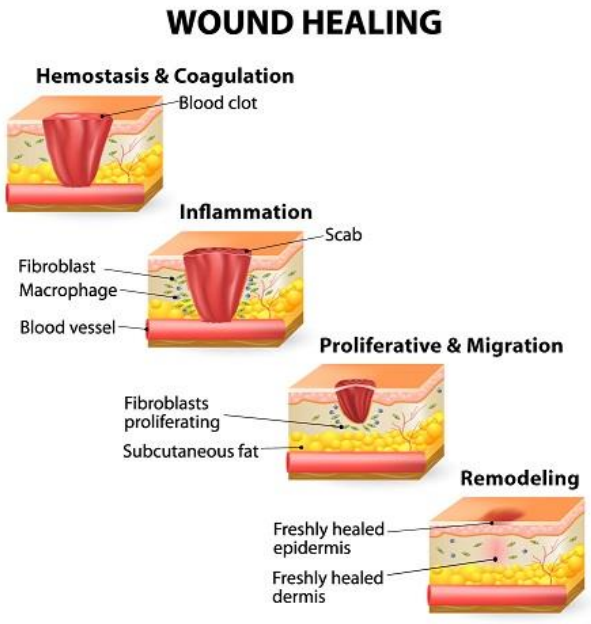

Figure 1.8 Steps of wound healing [25]

c) Proliferative Phase:

Within a few days of the original injury, the proliferative phase starts and can extend for a few weeks. New tissue is produced during this stage to replace the harmed tissue. Fibroblasts are specialized cells that move to the site of the wound and multiply to deposit new matrix. They are responsible for the production of collagen and other extracellular matrix components. Endothelial cells multiply and form new blood vessels to supply nutrients and oxygen to the healing tissue. Epithelial cells migrate from the wound edges and cover the wound's surface. This phase is distinguished by the formation of pink, soft, and granular granulation tissue.

d) Maturation Phase:

The maturation phase is the last stage of wound healing and can last up to two years. The newly deposited collagen is remodeled, aligned, and cross-linked during this phase to restore the original tissue architecture and tensile strength. As new tissue replaces the granulation tissue, the wound shrinks and becomes less visible. This stage is distinguished by the formation of a scar made up of collagen and other extracellular matrix components. Proper wound care, including the use of appropriate dressings and medications, can promote optimal wound healing while also lowering the risk of complications.

1.2.4.4 Challenges in wound healing

There are several challenges in wound healing, some of which include:

1. *Chronic wounds:* Chronic wounds are those that do not heal within a reasonable time frame, which is usually three months. These wounds are frequently linked to underlying medical conditions like diabetes, vascular disease, and obesity. Chronic wounds can be difficult to treat and may necessitate specialized care.

2. *Infection:* Infection is a common complication in wound healing. Bacteria can enter the wound and form biofilm (shown in Figure 9), which are bacterial communities embedded in extracellular polysaccharides and other polymers and adhered to a living thing or an inert surface. Due to their innate resistance to antibiotics and host immune

responses, biofilm is to blame for the persistence and clinical recurrence of some chronic wound infections.

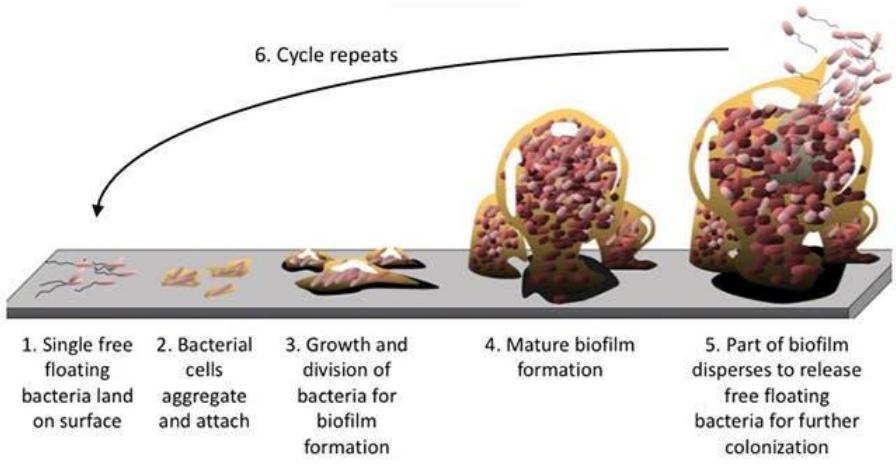

Figure 1.9 Process of formation of biofilm on a surface [26]

3. *Impaired circulation:* good circulation is necessary for wound healing. Impaired circulation, as seen in conditions such as peripheral arterial disease, can impede recovery and raise the possibility of problems.

4. *Poor nutrition**:*** Ample nutrition is essential for wound regeneration. Malnutrition or insufficient diet can delay healing and increase the risk of infections.

5. *Scar formation:* Scarring is a natural part of wound healing, but excessive scarring can cause functional and cosmetic problems. Scars can also be painful and itchy.

6. *Foreign bodies:* Foreign bodies such as dirt, debris, and sutures can interfere with the recovery process and raise the danger of infections.

1.2.4.5 Wound dressings

Wound dressings that promote rapid wound healing are necessary to inhibit microbial infection. No matter how big or small the wound, it needs to be treated properly. Since wound dressings are made to be in contact with skin, they are used for this purpose based on the type of wound. The use of wet-to-dry wound dressings, such as strips of linen

soaked in oil, was common in ancient times to treat wounds. Wool was dressed on wounds after being boiled in either water or honey or milk for wound cleaning. Highly porous, permeable to air, a barrier against microbes, and biocompatible wound dressings are ideal. Additionally, dressings must not be cytotoxic, absorb exudate, be allergic-free, and provide moisture for healing and peeling without causing any harm. Classes of wound dressings include hydrogel films, hydrocolloids, alginates, foams, and electrospun dressings. Electrospun sheets loaded with drugs are significant.

1.2.4.5.1 Drug-loaded electrospun sheets

Drug-loaded electrospun wound dressings are wound dressings that are designed to release therapeutic drugs or active agents into the wound site. They are produced by dissolving the drug in a polymeric solution and then electrospinning the solution.

The importance of drug-loaded electrospun wound dressings is based on their ability to deliver therapeutic drugs or active agents directly to the wound site, allowing for targeted and localized treatment. This targeted drug delivery system has the potential to reduce systemic toxicity and side effects associated with systemic drug administration while also improving treatment efficacy. Furthermore, electrospun wound dressings have a high surface area-to-volume ratio, allowing for more drug to be loaded onto the dressing and the ability to tailor the drug emission rate to the specific needs of the wound. Drug-loaded electrospun wound dressings have the potential to improve wound healing outcomes, reduce treatment time, and increase patient comfort, making them an important and promising research area in wound care.

1.2.4.5.2 Drug and its significance

Ciprofloxacin HCl (CIP), also known as ciprofloxacin hydrochloride, is an antibiotic medication that belongs to the fluoroquinolone class.

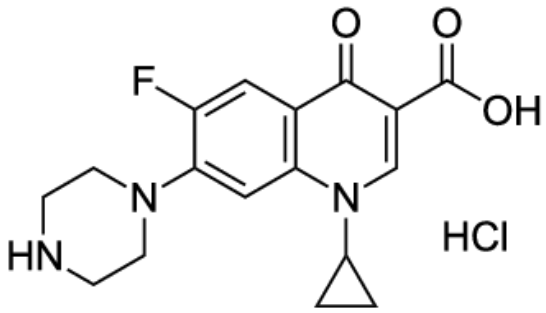

Figure 1.10 Chemical structure of ciprofloxacin hydrochloride

It is used to treat a wide range of bacterial infections, including those of the digestive tract, skin, urinary tract, and respiratory tract. Ciprofloxacin HCl works by inhibiting the activity of bacterial enzymes involved in the synthesis of bacterial DNA, thereby preventing bacterial growth and spread.

1.2.5 Nanotechnology

The fabrication of wound dressings with antimicrobial properties is currently the main focus. In order to prevent infections with multi-resistant antibacterial agents, nanomaterial-based antibacterial wound dressings are regarded as a successful strategy. Nanotechnology has gained popularity because of the nanoscale (1-100 nm) and surface adaptability of nanomaterials, which aid in penetration to kill microbes at the infectious wound site. Most antibacterial agents that can kill pathogenic bacteria have been created using nanomaterials. Nanomaterials like metal and metal oxide nanoparticles are primarily used as antibacterial agents for wound healing.

1.2.5.1 Nanoparticles

Nanoparticles (NPs) exhibit unique characteristics from their source materials and range in size from 10 to 1000 nm. Nano-particles can effectively deliver the drug in close contact with microbial colonies and offer controlled drug release, increased drug stability against harmful biofilm environments, and higher penetration in the biofilm. Indeed, it

has been shown that NPs increase antibiotic exposure to biofilm-embedded bacterial colonies and have the potential to prevent bacterial tolerance. Because of their small size, they are especially well-suited for wound healing.

Antibacterial wound dressings based on nanomaterials are regarded as a viable alternative to antibiotics in the prevention of multi-resistant antibacterial infections.

1.2.5.2 Chitosan-based nanoparticles

Chitosan is a natural biological polymer derived from chitin, which can be found in the shells of crustaceans such as prawns and crabs. Chitosan has a number of appealing properties, including its ability to break down, coexist with biological systems, and lack of toxicity, making it an appealing material for drug delivery applications. When chitosan is used to make nanoparticles, it can improve the properties of the drug by preventing degradation, increasing solubility, and allowing for controlled release.

Chitosan-based nanoparticles have been studied for a variety of biomedical applications such as therapeutic delivery, gene delivery, and tissue engineering. Chitosan-based nanoparticles have the potential to deliver therapeutic agents to specific cells or tissues while minimizing side effects due to their biocompatibility and biodegradability. Furthermore, chitosan-based nanoparticles have been shown to increase drug cellular uptake and bioavailability, making them a promising platform for improving drug efficacy. Chitosan nanoparticles were created by ion gelation of chitosan and sodium tripolyphosphate (TPP).

1.2.5.3 Electrospun sheets loaded with nanoparticles

Electrospinning has been widely used to create fibres with diameters ranging from a few microns to nanometers. Because of their resemblance to the ECM of the skin, nanofibers have improved regenerative capacity. When compared to other conventional dressings, nanoparticles incorporated into nanofibers have produced outstanding results. Nanomaterials are applicable in a wide range of medical practicalities, including

anticancer and antibacterial materials, medical equipment, environmental remediation, and wound healing.

In the current study, the chitosan-based ciprofloxacin nanoparticles were synthesized and loaded onto the bilayered electrospun sheets for the sustained released of ciprofloxacin. A comparison of ciprofloxacin hydrochloride and ciprofloxacin-loaded chitosan-based nanoparticles loaded in the bilayered electrospun sheets for wound healing application was done. The polymers used for the first layers were cellulose acetate and polyurethane while the second layer was of polyvinyl alcohol, in which drug and nanoparticles were loaded. The nanoparticles and bilayered electrospun sheets were characterized by different techniques.

Chapter 2

Literature Review

Abdel et al. prepared Cellulose acetate (CA) based nanofibers. The goal of this study was to create nanofibers based on cellulose acetate (CA) for use as drug transport for chronic wound healing. CA and polyethylene oxide (PEO) were combined for the first time. MB was mixed into random single layer CA/PEO nanofibers. Ciprofloxacin (Cipro) was introduced into a novel tri-layered aligned nanofiber made of CA/PEO that was surrounded by a blank layer of silk fibroin. This study concluded that CA electrospun nanofibers loaded with drugs might be useful in the treatment of chronic wounds. [27]

Teixeira et al. created a nanostructured mat that could kill bacteria while also promoting a healing environment for future wound care. At various polymer ratios, polyvinyl alcohol (PVA) and cellulose acetate (CA) were mixed. The antimicrobial peptide tiger 17 was loaded in CA.PVA nanofibrous sheet. Because of their moderate hydrophilicity and permeability, swelling capacity, and good peptide loading yields, crosslinked 90/10 PVA/CA mats were rated the most promising combination. [28]

Elsayed et al. discussed the synthesis of new biocompatible, biodegradable polymeric systems in this study. To regulate the blend's hydrophobicity/hydrophilicity ratio and subsequently enhance its biological contact with fibroblasts, these systems contained hydrophobic PLA coupled with either hydrophilic cellulose acetate polymer (CA) or poly (ethylene oxide) polymer (PEO). Nanofibrous dressing mats were created with sulfonamide included. Through enhanced epithelization, anti-inflammation, angiogenesis, and collagen deposition that exceeded commercially available ones, in-vivo testing demonstrated a considerable improvement in wound healing capacity [29].

Lemraski et al electrospun copper-containing nanofibers with chitosan and PVA and added polyvinylpyrrolidone as a secondary layer. The fibers were characterized using different techniques. *S. aureus* and *E. coli* were tested for antibacterial activity. The healing of samples was observed using rat open wounds. Various formulations were used.

These dressings proved to be antimicrobial and useful in the early steps of wound healing.

Vashisth et al. made a hydrophilic scaffold for skin restoration using a blend of PVA and gellan (PVA/gellan). Gellan, as a natural polymer, has good qualities for this purpose, such as degradability, compatibility, and aqueous adsorption, making it an appropriate choice for TE. PVA reduced the polymer repulsive forces in the blend, resulting in the creation of homogenous nanofibers. Cell culture experiments with human skin fibroblast revealed that these new scaffolds enhance cell attachment and proliferation more than traditional gellan hydrogels and dry films[30].

Adeli et al. synthesized a nanofiberous PVA/chitosan/starch scaffold with a carbohydrate-based biopolymer consisting of amylose (20%-30%) and amylopectin (70%-80%) and endowed with biocompatible, biodegradable, nontoxic, plentiful, and cost-effective qualities. The hybrid formulation revealed an exceptional ability to maintain the moisture needed for wound repair, with appropriate water uptake and moisture vapor transmission rates, as well as to shield the injured area from extrinsic influences throughout the healing process. The scaffold exhibited remarkable antimicrobial action against G-negative (Escherichia coli) and G-positive (Staphylococcus aureus) pathogens. Furthermore, in vitro cell toxicity assays showed appropriate cytocompatibility and cell viability confirming this polymer combination's remarkable potential for wound healing[31].

Unnithan et al. combined PU with cellulose acetate and zein to create innovative dressings to prevent infections and promote wound healing. The hydrophilicity of the dressings was improved, as was cell growth, attachment, and blood clotting. The antibiotic streptomycin was added to make them antimicrobial. The addition of cellulose and zinc improves the hydrophilicity of PU nanofibers, resulting in faster healing and a moist environment at the wound site [32].

Munoz-Escobar et al created antibacterial dressings for chronic wounds by incorporating copper nanoparticles into polymeric biomaterials such as polycaprolactone and polyurethane. They used disc diffusion and spectrophotometric methods to evaluate prepared dressings against six different bacterial strains. Antibacterial dressings were

found to have high antibacterial action. Thus, presenting a low cost, simple, fast, and potential candidate for chronic wound healing [33].

A.R. Unnithan et al. formed PU nanofibrous mats by combining hydrophilic dextran and hydrophobic PU. Ciprofloxacin, an antibiotic, was added to the mats to make them antibacterial. This combination resulted in mats with the required morphology. The materials were analyzed using a variety of procedures. Interaction between samples and fibroblasts was used to measure cell viability, attachment, and proliferation, and positive results were achieved. Furthermore, significant antibacterial activity was investigated. These characteristics make them excellent candidates for dressings [34].

Makvandi et al discussed several methods for incorporating nanomaterials into biological applications such as tissue engineering, wound healing, dentistry, and delivery systems. They investigated nanoparticles' potential as antibacterial and anti-biofilm agents[35].

Viembala et al. discussed the importance of copper nanoparticles as antibacterial agents. Cu/NPs have been utilized successfully in chronic wound dressing to prevent infection[36].

Chapter 3

Materials and Methods

2.1 Chemicals

Cellulose acetate (CA) of Molecular weight= 30kDa, degree of substitution (DS) = 2.4, and acetyl content~39.8% was purchased from Sigma Aldrich along with the Polyvinyl alcohol (PVA) (Mw~72kDa) and Ciprofloxacin hydrochloride (CIP) (≥ 98%). Poly-ether polyurethane (PU Z9A1) (Mw~197kDa), constituted 4,4-diphenylmethane diisocyanate, polyether diol, and 1,4-Butane diol was acquired from Biomer Technology, UK. Chitosan (CS), sodium tripolyphosphate (TPP) and sodium hydroxide (NaOH) were supplied by Sigma Aldrich Co. (USA). Acetone (99.8%) was bought from the BHD AnalaR NORMAPUR. N, N-Dimethylacetamide (DMAc) was provided by UNI-CHEM Chemical Reagents. Acetic acid (99.8%) was delivered by BHD AnalaR Laboratory supplies, England. All the chemicals used were analytically pure and used as it is.

2.2 Methods

2.2.1 Electrospinning

The technique used to make the nanofibrous sheets with different compositions was electrospinning. Electrospinning is an efficient method to produce fibers going from nanometers to micron meters in diameter that are used in various fields such as tissue engineering, drug distribution, wound dressings, filtration, food, and packaging industries.

The bilayer electrospun sheets were fabricated by using Electro-spinning & Spray unit (China), model number TL-01 with a supply voltage~AC 220V, power frequency~50-60Hz, power rating~700W and high voltage module of max. +50kV.

The components of electrospinning are a high-voltage supply unit, a metal collector, a needle attached to a syringe, and a significant electrical potential difference applied between the needle and metal collector.

Figure 3.1 Electro-spinning & Spray unit (China), model number TL-01

2.2.2 Preparation of solutions for electrospinning

To prepare the 23%w/v cellulose acetate (CA) solution, CA has been dissolved in acetone/DMAc (1:2) solvent mixture [37], being continuously stirred at 200 rpm using a magnetic stirrer (CORNING PC-420D) at room temperature to obtain a clear solution. Polyether-polyurethane (PU) was mixed in acetone/DMAc (1:2) to get a concentration of 15%w/v, by placing the solution on a magnetic stirrer in a water basin at the temperature of 45°C. Polyvinyl alcohol (PVA) with a concentration of 8%w/v was made by solubilizing PVA in distilled water while 5%w/v ciprofloxacin powder (wt.% w.r.t polymer weight altogether) was added to the above prepared 8%w/v PVA solution to get a homogeneous mixture. All the concentrations were adjusted after the various optimizations of each component.

2.2.3 Fabrication of nanoparticles

Ciprofloxacin loaded chitosan-based nanoparticles were fabricated using ion gelation method. In order to make chitosan solution 1% chitosan was dissolved in 10 mL of 1% (v/v) acetic acid solution, and the mixture was agitated until a clear solution was produced. The pH of CS solutions was adjusted to 5 by adding a few drops of (1M)

NaOH solution. Preparation of ciprofloxacin solution was done separately by adding ciprofloxacin in distilled water. The ciprofloxacin solution was poured into the chitosan solution drop by drop, over an hour of magnetic stirring. 100 mL of 0.1% (w/v) TPP solution was incorporated dropwise into the chitosan-ciprofloxacin (CS-CIP) solution while stirring. The solution was stirred for 4 hours to complete the ion gelation process, resulting in the formation of ciprofloxacin-chitosan nanoparticles (CIP NPs).

The nanoparticles were collected by centrifugation at 15,00 rpm for 15 minutes and washed with distilled water several times. The nanoparticles were then analyzed by techniques such as IR spectroscopy, and zeta potential measurements [38].

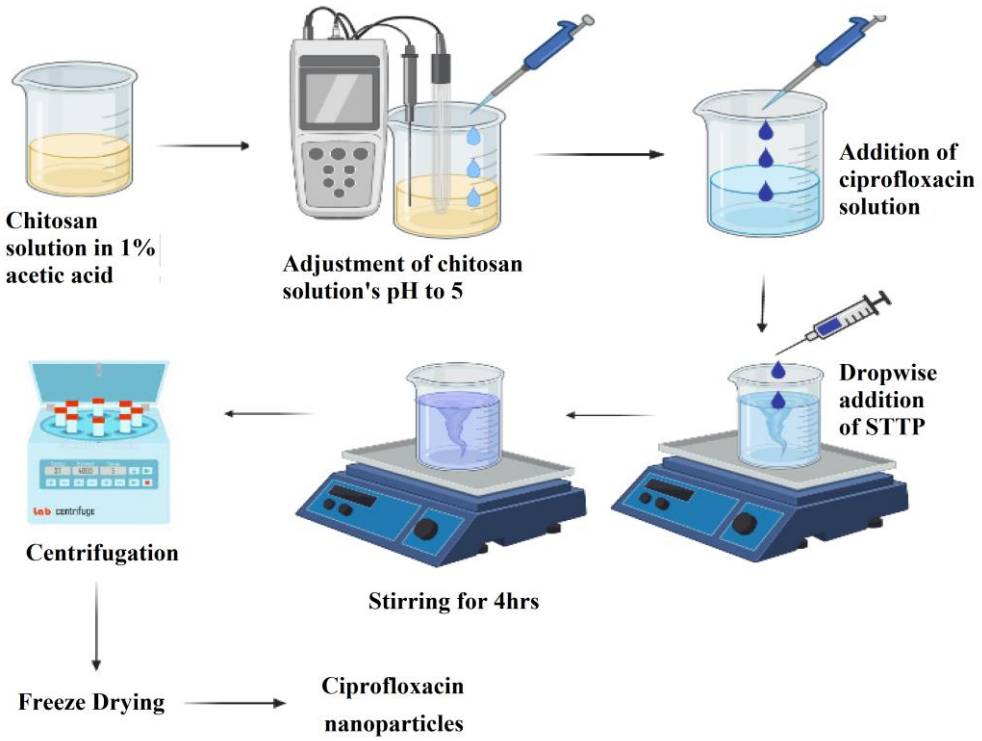

Figure 3.2 Preparation of Ciprofloxacin nanoparticles (CIP NPs)

2.2.4 Fabrication of electrospun sheets

The nanofibrous sheets of cellulose acetate, polyvinyl alcohol and polyether polyurethane were optimized separately at first as control sheets. After trying many concentrations, the optimized control sheets were developed in following concentrations, 23 % w/v of

cellulose acetate, 15% w/v of polyurethane and 8%w/v of polyvinyl alcohol. The fabricated compositions in this study are shown in table 1. The optimized parameters for the polymers control sheets are shown in table 2.

Table 3.1 Fabricated electrospun sheets

Composition name	Abbreviations
Precursor sheets	
Cellulose acetate	CA
Polyurethane	PU
Polyvinyl alcohol	PVA
Cellulose acetate + Polyurethane (6: 4)	CA/PU (6:4)
Cellulose acetate + Polyurethane (8:2)	CA/PU (8:2)
Composite sheets with ciprofloxacin	
Cellulose acetate + Polyurethane (6: 4) bilayered with Polyvinyl alcohol + ciprofloxacin	CA/PU (6:4): PVA (CIP)
Cellulose acetate + Polyurethane (8: 2) bilayered with Polyvinyl alcohol + ciprofloxacin	CA/PU (8:2): PVA (CIP)
Composite sheets with nanoparticles	
Cellulose acetate + Polyurethane (6: 4) bilayered with Polyvinyl alcohol + ciprofloxacin nanoparticles	CA/PU (6:4): PVA (NPs)

Table 3.2 Optimized conditions for CA, PVA, PU, CA/PU (6:4), and CA/PU (8:2)

Polymers	Concentrations (%w/v)	Flowrate (ml/h)	Needle gauge (G)	Voltage (kV)	Distance from needle tip to collector
CA	23%	0.5	21	17	10
PVA	8%	0.1	20	12	10
PU	15%	0.1	20	16	10
CA/PU	(6:4)	0.1	20	15	12
CA/PU	(8:2)	0.1	20	15	12

2.2.5 Fabrication of electrospun sheets incorporated with ciprofloxacin

For the first layer of the electrospun sheet, solutions of CA and PU were prepared separately, then mixed in ratios (6:4 and 8:2) to produce CA/PU sheet. PVA solution was made separately, and then ciprofloxacin was incorporated into the prepared PVA solution to formulate the blend for the bilayer on both compositions.

First layer: The 23% w/v CA solution and 15% w/v PU were combined in 6:4 and 8:2 ratios using the magnetic stirrer at 200 rpm for 1 hour to get a homogeneous solution. The solution of CA/PU was added to the 20 ml disposable plastic syringe. A stainless steel 20 G needle with an inside diameter of 0.603 mm was fitted to the syringe. At a voltage of 15kV, the solution was pushed through a syringe pump (Spray Unit TL-01) at the rate of 0.1ml/h. The needle-to-collector distance was kept constant at 12 cm. The fibers were collected on the glossy sheets wrapped around the rotating drum collector. After the collection of fibrous sheets, they were dried for 24h to remove the excess solvent [39], [40].

Second layer: The 8%w/v PVA solution with added 5% ciprofloxacin powder was spun on the first layer prepared in the above procedure [41]. The solution of PVA/CIP was added to the 20ml disposable plastic syringe. The syringe was fixed to a stainless steel 20G needle with an inner diameter of 0.603 mm. The solution was pumped through the syringe pump (Spray Unit TL-01) with a rate of 0.1ml/h at a voltage of 15kV. The distance between the needle to collector was kept at 12 cm [42]. The fibers were collected on the above-prepared CA/PU sheets wrapped around the rotating drum collector. The final sheets obtained were CA/PU (6:4 and 8:2) coated with PVA loaded with ciprofloxacin [CA/PU (6:4): PVA (CIP)] and [CA/PU (8:2): PVA (CIP)]. After the collection of fibrous sheets, they were dried for 24h to remove the excess solvent.

Table 3.3 Optimized conditions for CA/PU (6:4): PVA (CIP), CAPU (6:4): PVA (NPs), CA/PU (8:2): PVA(CIP)

Polymers	Flowrate (ml/h)	Needle gauge	Voltage (kV)	Distance from needle tip to

		(G)		collector (cm)
CA/PU (6:4): PVA (CIP)	0.1	20	15	12
CAPU (6:4): PVA (NPs)	0.1	20	15	12
CA/PU (8:2): PVA(CIP)	0.1	20	15	12

2.2.6 Fabrication of nanoparticles loaded electrospun sheets

Following the above procedure that was used to make ciprofloxacin incorporated sheets, the sheets with ciprofloxacin nanoparticles were produced. The first layer of cellulose acetate and polyurethane were same as mentioned above and for the bilayer ciprofloxacin nanoparticles were added into polyvinyl alcohol.

5% of CIP NPs (according to polymers weight) were added in PVA solution and stirred until a homogenous solution was formed. The solution was then electrospun with the following parameters: needle 20 G flowrate was 0.1ml/h, voltage was 15kV, and the distance between the tip of needle to the collector was kept at 12cm. The nanofibers were collected on the CA/PU (6:4) sheet which was formed before. Hence CA/PU sheet bilayered with PVA loaded nanoparticles [CA/PU (6:4): PVA (NPs)] was developed. After the collection of fibrous sheets, they were dried for 24h to remove the excess solvent [43].

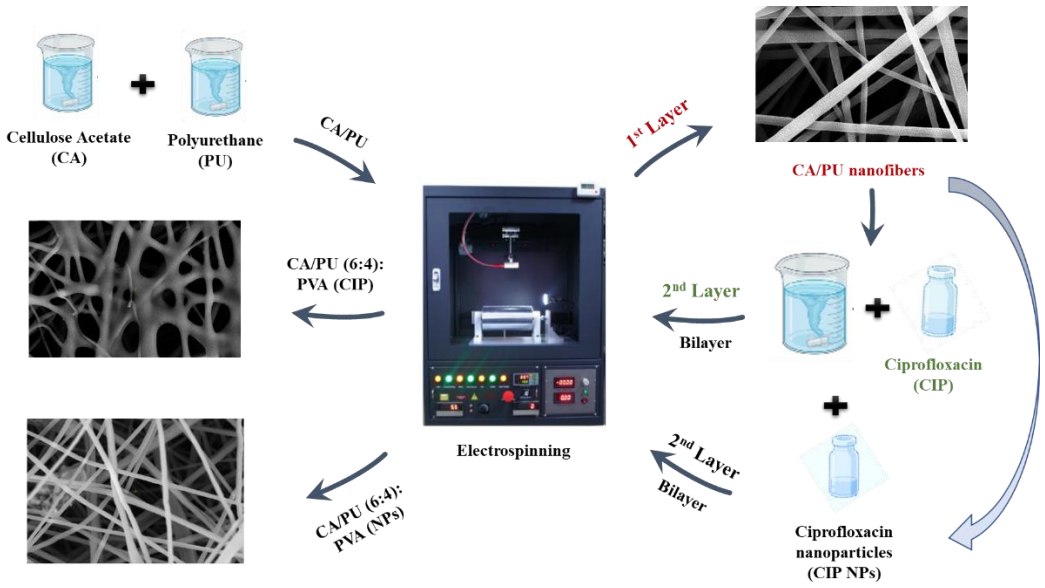

Figure 3.3 Preparation of CA/PU, CA/PU: PVA (CIP), and CA/PU: PVA (NPs) electrospun sheets using electrospinning

2.3 Characterizations of nanoparticles

The formulated nanoparticles were studied by using FTIR and zeta measurements. The ATR FT-IR spectrum of the prepared nanoparticles was recorded using an FT-IR spectrophotometer (Thermo Nicolet Scientific 6700 FTIR, USA) having a scanning range of 4000-400 cm^{-1}, a spectral resolution of 128 cm^{-1}, and a total of 8 scans [38]. It was used for confirmation of nanoparticle formation and the chemical combination that exists between the different components of the nanoparticles by analyzing the characteristic peaks of chitosan and ciprofloxacin. A Zetasizer instrument was used to determine the mean particle size (Z-average), poly-diversity index PDI, and Zeta Potential of CIP NPs.

2.4 Characterizations of electrospun sheets

The prepared electrospun sheets with cellulose acetate and polyether-polyurethane coated with polyvinyl alcohol loaded with ciprofloxacin and nanoparticles, were studied using several characterizations.

2.4.1 Field Emission Scanning Electron Microscopy (FESEM)

Field Emission Scanning Electron microscopy (FESEM, Apreo S Lo Vac, Thermofischer Scientific, Netherland) was exploited to see the surface and sectional morphology of the electrospun sheets, including fiber diameter and alignment. Using a sputter-coated apparatus, a tiny layer of gold was sputter-coated onto the samples before imaging to enhance surface conductivity. The microscope was set to an acceleration voltage of 20 kV. FESEM images taken at different magnifications provide information about the overall structure and morphology of the electrospun sheets. The images were analyzed through the ImageJ software to get the diameter of the fibers [44].

2.4.2 FTIR Spectroscopy

FTIR Spectroscopy was used to examine the chemical composition of the electrospun sheets. A Thermo Nicolet Scientific 6700 FTIR, USA was used for the spectra of polymeric sheets.

Figure 3.4 A Thermo Nicolet Scientific 6700 FTIR, USA instrument for evaluation of functional groups

The Attenuated Total Reflection (ATR-FTIR) mode with a resolution of 128 cm^{-1}, a range of 4000-400 cm^{-1}, and 8 scans. was utilized to analyze the control and composite sheets.

2.4.3 X-Ray structural analysis (XRD)

The crystal structure of the electrospun sheets was explored using Rigaku MiniFlex 600C X-ray Diffractometer with HYPIX-400 MF 2D hybrid pixel array detector. Cu anode, Ka radiations in the Bragg-Bentano configuration with 0.02 (20) step size per 0.05s was used. This technique provides information about the size of the crystals and their level of crystallinity in the different b components in the electrospun sheets [44].

2.4.4 Thermogravimetric measurements (TGA)

Thermogravimetric measurements (TGA) were done to determine the temperature durability and degradation behavior of the electrospun sheets using BXDSC-TGA-1250 (BAXIT China). The experiments were carried out in a nitrogen environment that was continuously present at a heating rate of 10 °C/min from ambient temperature to 700 °C. Weight loss as a function of temperature was measured. Information regarding the heat stability and breakdown temperature of the sheets is available from TGA curves.

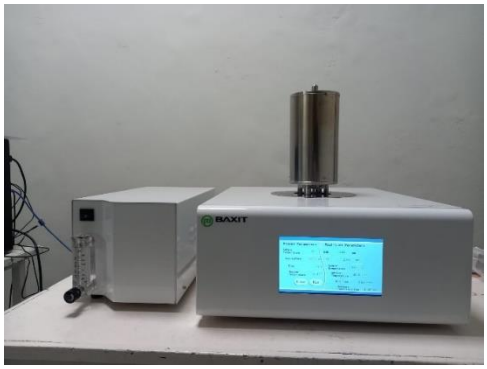

Figure 3.5 BXDSC-TGA-1250 (BAXIT China) for thermogravimetric analysis

2.4.5 Wettability / Contact Angle measurements

Biolin Scientific Attention Theta Flex instrument was used for surface wettability analysis of the electrospun sheets.

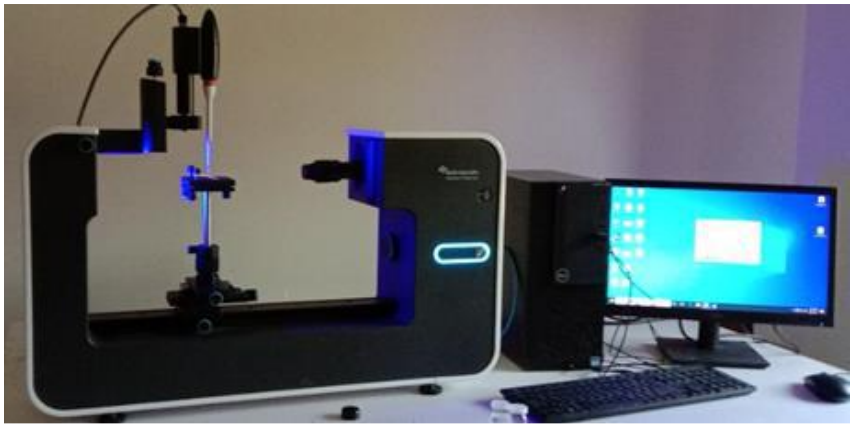

Figure 3.6 Biolin Scientific Attention Theta Flex instrument for surface wettability analysis

The sessile drop technique was employed, samples were placed on a contact angle meter, and a 40 µL distilled water droplet was placed on the surface with a tip of 200 µL. The droplet's angle of contact with the surface was measured and the images were taken by the camera [44].

2.4.6 Density measurements

The density of the fabricated electrospun sheets was evaluated by using the pycnometer (PENTAPYC 5200e Automatic Density Analyzer).[45]. The parameters provided for the density measurements were target pressure of 19P with 6 number of runs and 3 average runs.

Figure 3.7 Pycnometer (PENTAPYC 5200e Automatic Density Analyzer) for density measurements

2.4.7 Dynamic Mechanical Analysis (DMA)

Mechanical characterization of the materials was conducted using the TA instruments Dynamic Mechanical Analysis (DMA) system, specifically the DISCOVERY DMA 850 model. The stress-strain curve of the fabricated sheets was obtained by DMA. The stress-strain curve was obtained by using a pre-load of 10N at room temperature.

2.4.8 Antibacterial assay

Disc diffusion was used to assess the antibacterial activity of all composite sheets including free drugs and nanoparticles against Escherichia coli (*E. coli*) and Staphylococcus aureus (*S. aureus*). 100ul of bacterial strain were placed in 10 ml of LB broth, and the inoculum was maintained at 37 °C for 24 hours to obtain the bacterial strains. The inoculum's optical density was kept at 0.1 (using UV spectrophotometer) with LB media after 24 hours. A 100ul culture was distributed from the inoculum onto agar-solidified petri plates before samples (composite sheets) were added to the plates. The drug and nanoparticle solution were taken as a positive control and the control sheets without the drug or nanoparticles were used as negative control. For the solutions, agar was cut into wells for the well diffusion procedure, and 20 ul of the drug solution and suspension of nanoparticles were applied to each well. After 24 hours, the plate's inhibition zone on the plates was measured using a scale [46].

2.4.9 Drug release study

The protocol described in the literature for investigations on the release of drugs from nanofibrous mats has been applied [47]. Each of the ciprofloxacin-infused nanofiber mats was divided into pieces (containing drug weight ~5 mg) and stored in a glass vial containing 15 mL of PBS (pH 7.4). The glass vials were kept at 37C with aluminium foil on top of them. At regular intervals, 5 mL of PBS was removed and replaced with the same volume of fresh media. The standard calibration curve was used to determine the concentration of ciprofloxacin released from the nanofibrous mats, and the release profiles were shown as percentage drug release v/s time [48].

Chapter 4

Results and Discussions

Electrospun sheets of cellulose acetate (CA), polyvinyl alcohol (PVA), polyether polyurethane (PU), CA/PU, and CA/PU: PVA (CIP) were successfully prepared using electrospinning technique.

3.1 Characterizations of nanoparticles

The nanoparticles of ciprofloxacin were also analyzed by FTIR and Zeta measurements.

3.1.1 FTIR

The capacity of FTIR (Fourier-transform infrared) spectroscopy to provide useful information about the chemical composition, functional groups, and molecular structure of nanoparticles makes it a powerful approach for their analysis.

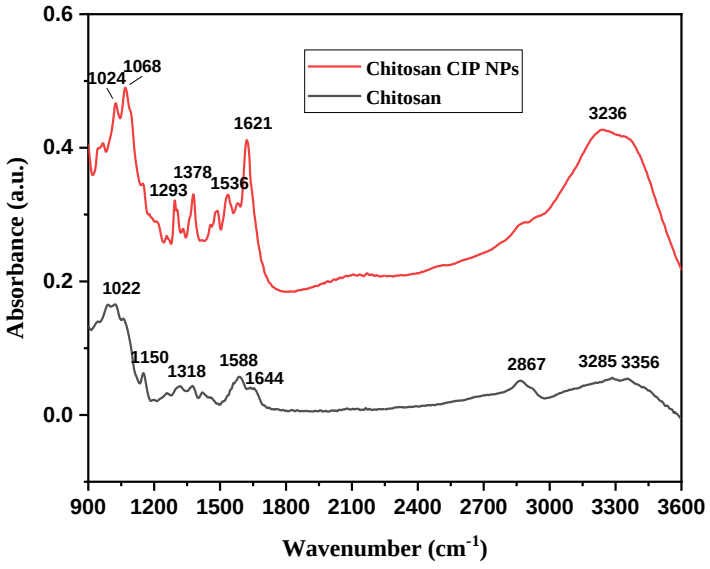

Figure 4.1 FTIR analysis of chitosan and synthesized ciprofloxacin nanoparticles

The encapsulation of ciprofloxacin in chitosan-based nanoparticles was confirmed by FTIR analysis. The FTIR spectra of chitosan (CS) and chitosan-ciprofloxacin nanoparticles (NPs) are shown in Fig. (4.1). The absorption band at wavenumbers 3356 cm^{-1} and 3285 cm^{-1} in the chitosan spectra correlates with NH_2 and OH stretching vibrations. The peaks at 1644 cm^{-1} and 1588 cm^{-1} represent amide I (C=O) and amide II (N-H) respectively, and the peaks at 1318 cm^{-1} show vibrations of $C\text{-}CH_3$ and $C\text{-}NH_2$. 1150 cm^{-1} corresponds NH_2 bending, and 1022 cm^{-1} indicates C-O-C of glycosidic linkage in chitosan [38].

The FT-IR spectra of NPs display the same peak absorbance as CS along with shift. The NH_2 and OH group's vibration stretching bands appear at 3356 cm^{-1} and 3285 cm^{-1} in CS, whereas it relocates to 3236 cm^{-1} in NPs and becomes broader due to hydrogen bonding [49]. A shoulder peak at 1644 cm^{-1} in CS fades, while a new one develops at 1621 cm^{-1} in NPs. The stretching vibrations of the C=O bond in the amide group in both ciprofloxacin and chitosan cause this peak. This peak supports the existence of chitosan in the nanoparticles and implies that ciprofloxacin interacts with the chitosan matrix via hydrogen bonding or other intermolecular interactions. The bending vibration of NH_2 has shifted to 1536 cm^{-1} [50]. The bond peak at 1293 cm^{-1} corresponds to C-F group of ciprofloxacin confirming the nanoparticle formation [51]. The presence of chitosan and ciprofloxacin peaks confirm the formation of chitosan ciprofloxacin nanoparticles.

3.1.2 Zeta Measurements

The size and zeta potential of nanoparticles were evaluated using Zetasizer Nano ZS90 (Malvern, UK)

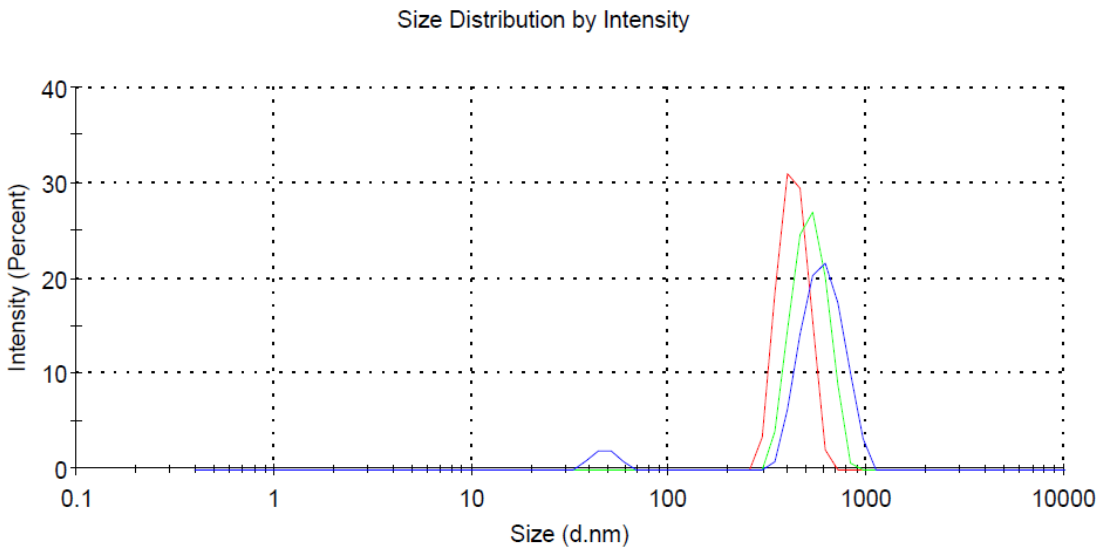

Figure 4.2 Zetasizer analysis of ciprofloxacin nanoparticles

The particle size of the generated nanosuspensions is a significant parameter [52]. The dynamic light scattering approach, which involves scattering a laser light beam at the surface of dispersed NPs and detecting the backscattered light, could be utilized to successfully measure these important parameters [53]. The results showed that the produced chitosan NPs hava a mean particle size of 539 nm with polydiversity of 0.343.

3.2 Characterizations of electrospun sheets

The morphology physical and chemical properties of the electrospun sheets were characterized using Field Emission Scanning Electron Microscopy (FE-SEM), Fourier IR Spectroscopy (FTIR), X-Ray Diffraction analysis (XRD), contact angle measurements, antibacterial activity, and drug release studies.

3.2.1 Field Emission Scanning Electron Microscopy (FE-SEM)

FESEM is a type of electron microscopy that uses a beam of electrons to create high-resolution images of the surface of a sample. FESEM works by emitting electrons from a sharp metal tip at the end of a vacuum-sealed chamber and focusing them onto the sample's surface with electromagnetic lenses. FESEM has several advantages over other types of microscopies, including high magnification, high resolution, and the ability to analyse samples in different environments (for example, vacuum, air, or liquid). As a result, it is useful in a variety of scientific fields, including materials science, biology, and nanotechnology. FESEM is frequently used to assess the morphology, appearance, and composition of materials such as metals, ceramics, polymers, and biological samples. It can also be used to analyze the surface of samples at various scales, ranging from nanometers to micrometres, and provide detailed information about surface features, defects, and properties. We used Field Emission Scanning Electron Microscopy (FE-SEM) to examine the configuration and surface topography of electrospun sheets made of cellulose acetate (CA), polyurethane (PU), polyvinyl alcohol (PVA), and their blends with ciprofloxacin and ciprofloxacin nanoparticles.

We used Field Emission Scanning Electron Microscopy (FESEM) to characterize the morphology and surface topography of electrospun sheets made from chitosan CA, PU, PVA, CA/PU (6:4), CA/PU (8:2), CA/PU (6:4): PVA (CIP), CA/PU (8:2): PVA (NPs). The electrospun sheets had a fibrous structure with a smooth surface, as revealed by FESEM images. The CA and PVA electrospun sheets, PU, CA/PU (6:4), and CA/PU (8:2) electrospun sheets had uniform and smooth surfaces, whereas the blended electrospun sheets, CA/PU: PVA (CIP), had thick fibres and CA/PU (8:2): PVA (NPs) particles

attached to the fibres. This morphological difference was attributed to the viscosity of the polymers used, which can affect the fiber formation process during electrospinning. The addition of PVA and ciprofloxacin caused the increase in diameter from 194 to 261 nm of the electrospun sheets, with the presence of PVA resulting in a smoother surface and the presence of ciprofloxacin resulting in a slightly rougher surface with some aggregated particles visible on the fibers.

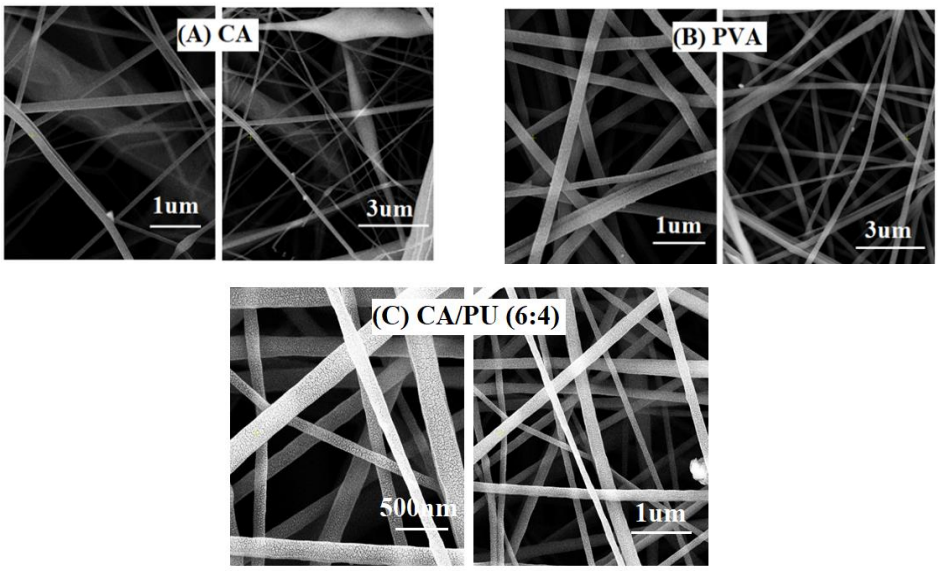

Figure 4.3 FESEM images of (A) CA, (B) PVA, (C) CA/PU (6:4), at 1um, 3um at magnification of 50,000

FESEM images revealed that the electrospun sheets of had different fibrous structures. The CA sheet showed the morphology of fibers that are smooth and average in diameter of 171 ± 0.06 nm and the fibers were not uniform [44]. PVA sheet had a uniform and smooth fibrous structure with a typical diameter of 214 ± 0.04 nm [54]. The CA/PU (6:4): PVA (CIP) showed thick fibers of 264 ± 63 nm diameter. The CA/PU (6:4): PVA (NPs) sheet had a mixed fibrous, non-uniform structure with a little agglomeration of fibers, having the average diameter of 125 ± 8.6 nm.

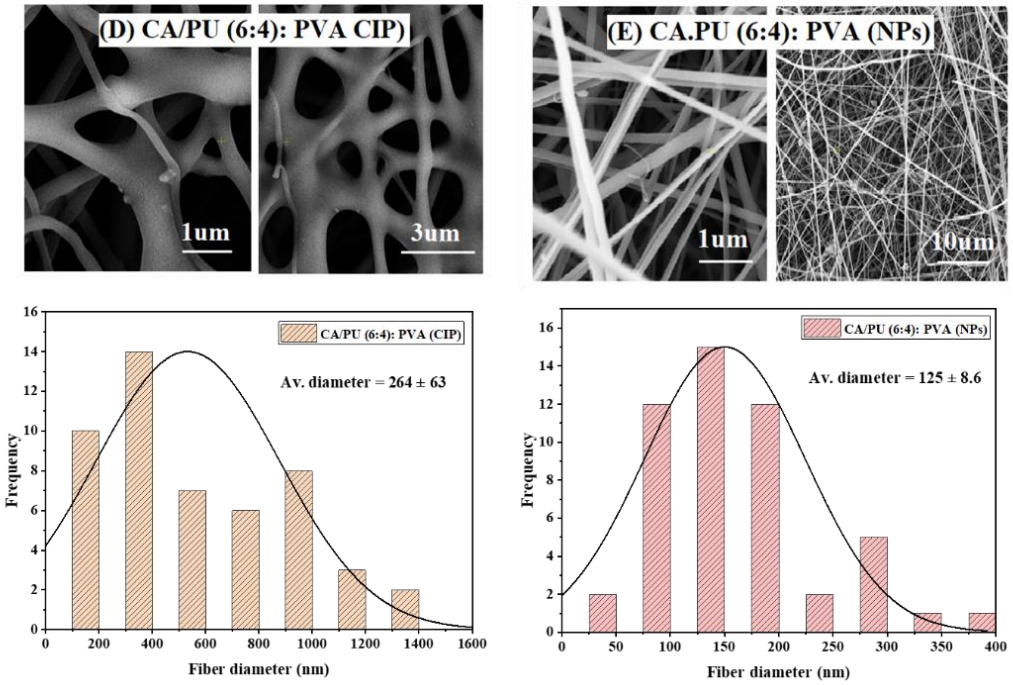

Figure 4.4 FESEM images of (D) CA/PU (6:4): PVA (CIP) (E) CA/PU (6:4): PVA (NPs) at 1um, 10um at magnification of 50,000

3.2.2 Fourier Transform Infrared Spectroscopy (FTIR)

FTIR technique was used to examine interactions between different functional groups of electrospun nanofibers. The FTIR of precursor sheets as well as composite sheets with free drug and nanoparticles are given below:

The FTIR spectrum of CA in figure 3.2 shows the characteristic peaks at approximately 1030cm^{-1}, 1218 cm^{-1}, and 1733 cm^{-1}, which correspond to the C-O-C bond elongation vibrations of cellulose backbone, symmetric stretching of C-O bond vibrations, and C=O of acetyl group respectively. The peaks present at 3468cm^{-1} and 2941cm^{-1} belong to the O-H stretching vibrations of the hydroxyl groups and C-H extension vibrations of the methyl group correspondingly, while the peaks seen at 1432 cm^{-1} and 1367cm^{-1} are caused by the C-H bending vibrations [55].

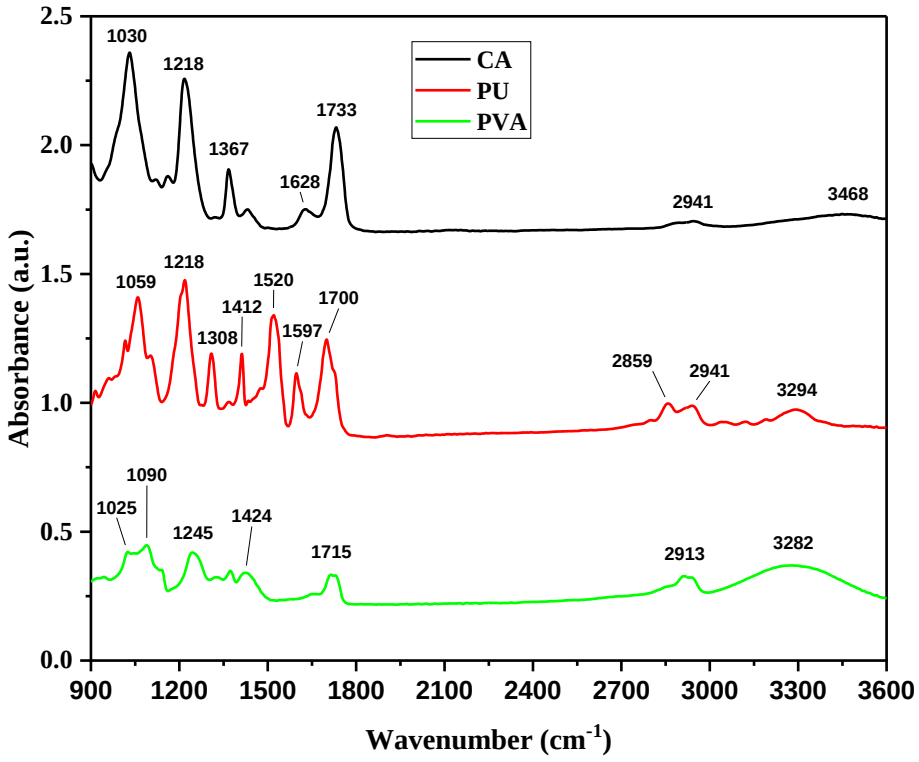

Figure 4.5 ATR-FTIR spectrum of CA, PU, PVA

In figure 4.5, PU spectrum proves the distinctive peaks at 1700cm^{-1} and 3294cm^{-1} related to the C=O and N-H in the urethane linkage (-NHCOO-). The peak located at 1520 cm^{-1} was assigned to N-H vibrations while 1597 cm^{-1} belongs to C-H vibrations. The peaks

seen at 2941 cm^{-1}, and 2859 cm^{-1} were of CH_2 and CH_3 stretching. A peak around 1218 cm^{-1} is the polyether polyol's C-O-C ether linkage stretching vibration. The peaks occurring at 1059 cm^{-1} and 1218 cm^{-1} are associated with the C-O bond vibrations in the ether while 1308 cm^{-1}, and 1412 cm^{-1} show the C=C of the benzene ring [56].

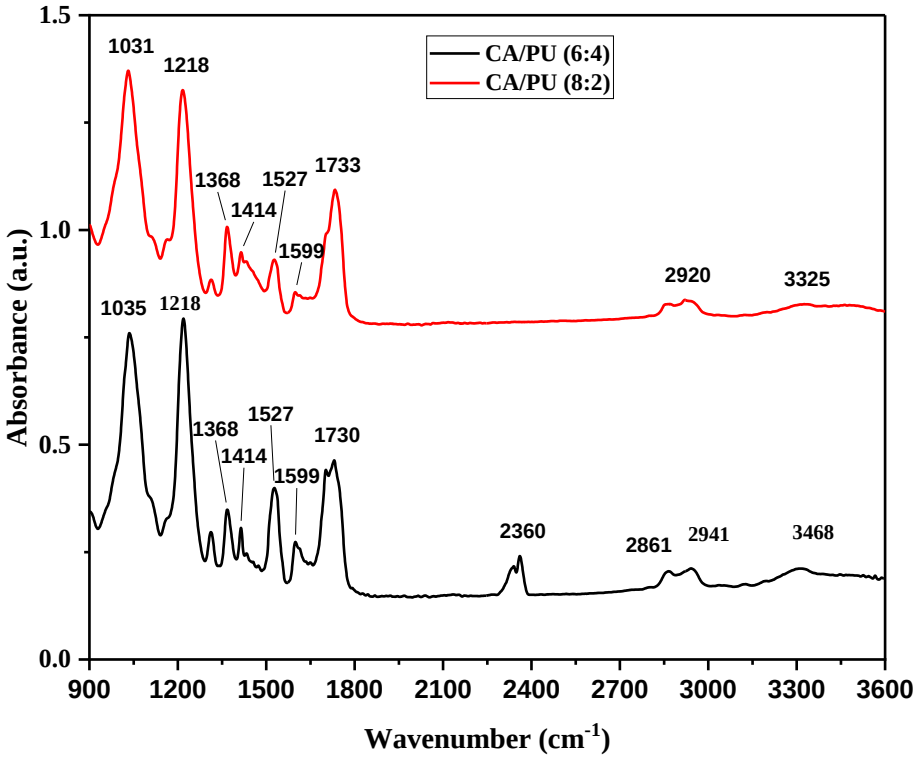

Figure 4.6 ATR-FTIR spectrum of precursor sheets [CA/PU (6:4) and CA/PU (8:2)]

After mixing CA/PU, the peaks observed for asymmetric vibration and bending vibration of CH_2 were at 2941 cm^{-1} and 1414 cm^{-1} respectively, and the peak representing the C=O stretching vibration in the carbonyl group can be seen at 1730 cm^{-1}. These absorption peaks are typical peaks of the same functional groups in CA and PU as shown in figure 3.4. Both the stretching-bending vibrations of N-H are responsible for the absorption peaks at 3309 cm^{-1} and 1599 cm^{-1}, correspondingly [40].

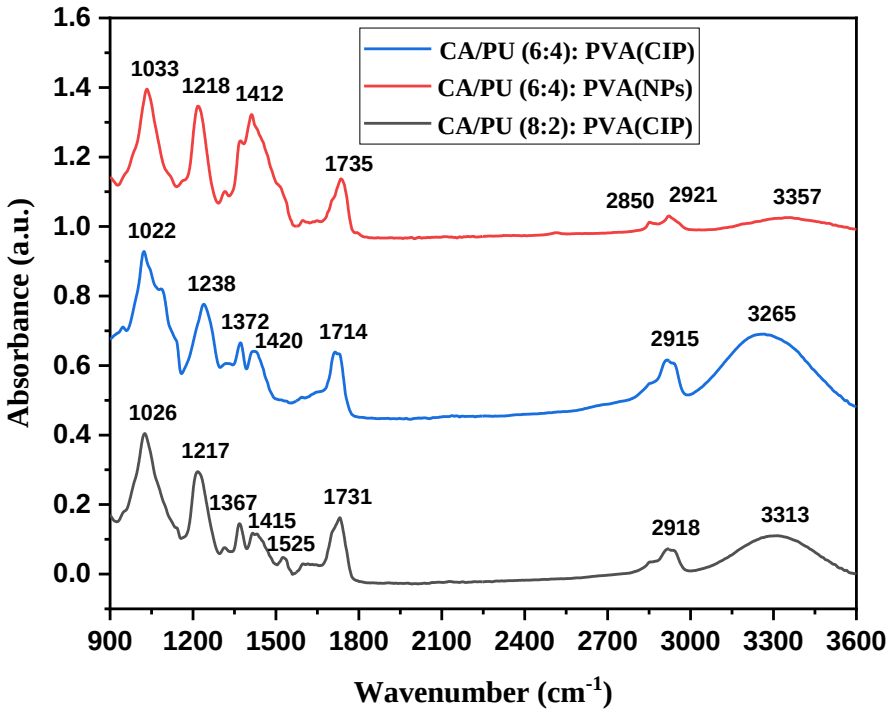

Figure 4.7 ATR-FTIR spectrum of CA/PU (6:4): PVA (CIP), CA/PU (8:2): PVA (CIP), CA/PU (6:4): PVA (NPs)

When PVA loaded with ciprofloxacin is bilayered on the CA/PU sheet [CA/PU: PVA (CIP)], the peaks of all the components were visible showing that there is physical interaction between the layers, and no new peak was formed. The peak corresponding to O-H present in PVA, and ciprofloxacin is prominent at 3313 cm^{-1} with increased intensity, and 2918 cm^{-1} belongs to the C-H stretch of polyurethane as well as ciprofloxacin. The C=O group present in all components showed a peak at 1731 cm^{-1}. The amplitude of the peak observed at 1217 cm^{-1} is due to C-O-C present in PVA as well as PU. 1025 cm^{-1} peak corresponds to C-O vibration. The peaks at 1368 cm^{-1} and 1415 cm^{-1} are attributed to C=C of the benzene ring and C-H bending vibrations, respectively [57].

The Fourier transform infrared (FTIR) spectra of bilayered electrospun sheets composed of the first layer of cellulose acetate (CA) and polyether polyurethane (PU), with a

second layer of PVA (CIP) and PVA (NPs), were analyzed to investigate the chemical composition and interactions between the components. The discussion of the FTIR analysis is presented below.

The FTIR spectra (shown in figure: 4.5) of the electrospun sheets revealed characteristic absorption peaks of both CA and PU, indicating their co-existence in the electrospun sheets. the carbonyl groups of CA and the urethane groups of PU. When cellulose acetate and polyether polyurethane are mixed together and undergo transesterification, the C=O stretching vibrations of the ester and urethane/urea groups overlap resulting in the increase in the intensity of the peak and a slight shift to 1730 cm^{-1} in the spectrum. This corresponds to the development of hydrogen bonding [40].

The FTIR spectra of the bilayered electrospun sheets with the PVA loaded ciprofloxacin sheet exhibited characteristic absorption peaks of all the components, indicating their co-existence in the electrospun sheets. Additionally, the spectra exhibited a slight shift in the peaks of CA/PU and PVA (CIP) sheet, suggesting some degree of interaction between the layers. The peak at 3282 cm^{-1} for PVA shifted slightly to 3265 cm^{-1} in the bilayered electrospun sheets, indicating the possible establishment of hydrogen bonds between the O-H group of PVA and the ester or urethane groups of CA/PU. The addition of ciprofloxacin to PVA results in vanishing of the 1621 cm^{-1} band, indicating a weakening of the carboxylic acid group. This could be due to hydrogen bonding between the carboxylic acid group of ciprofloxacin and the hydroxyl group (-OH) of PVA, which can disrupt the C=O stretching of the carboxylic acid group. The spectra of CA/PU (6:4): PVA (NPs) shows the same peaks but they are broader indicating that the nanoparticle peaks are shown in the same region [57], [40].

3.2.3 X-Ray Diffractometry (XRD)

A non-destructive analytical method used to investigate the crystal structure of materials is called X-ray diffraction (XRD). The method is based on the idea that when X-rays interact with the atoms in a material, they scatter in a particular pattern. A series of peaks that are indicative of the precise angles at which the X-rays are scattered make up the diffraction pattern. Information about the crystal structure of the substance can be gleaned from the locations and intensities of the peaks in the diffraction pattern. XRD of CA/PU (6:4), CA/PU (8:2) and bilayered electrospun sheets CA/PU (6:4): PVA(CIP), CA/PU (8:2): PVA(CIP), CA/PU (6:4): PVA(NPs) was done to investigate the amorphous or crystalline nature.

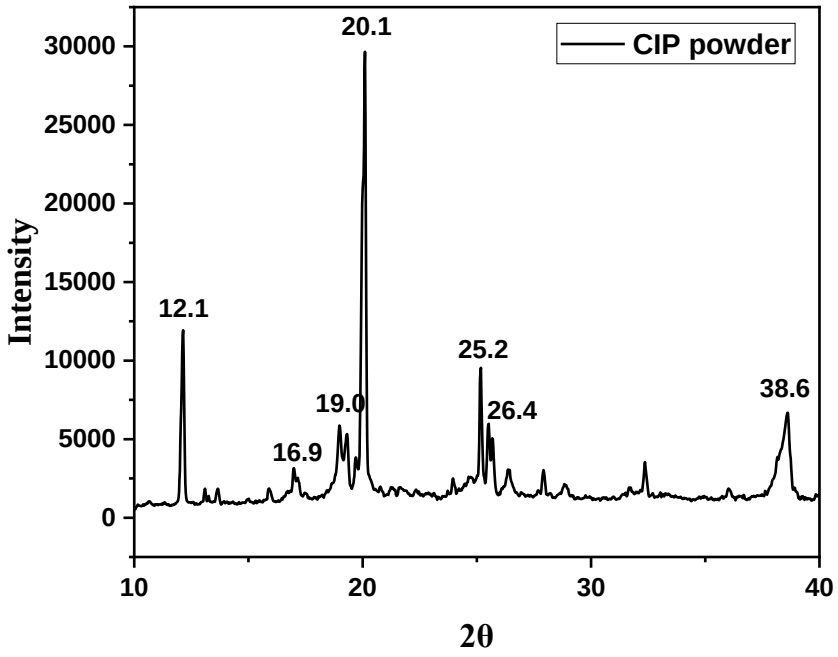

Figure 4.8 XRD spectra of pure ciprofloxacin powder

The graph (figure 4.9) shows the distinctive peaks of ciprofloxacin at 2θ = 12.1°, 20.1°, 25.2°, 26.4°, 38.6°, 16.9°, and 19.0 °, revealing the drug's regular crystal structure [58].

In general, cellulose acetate is a semi-crystalline material, with both crystalline and amorphous regions. The amorphous nature of cellulose acetate is demonstrated by the two wide peaks at 2θ= 10° and 2θ=18° [59]. A typical broad peak at 19.4°, which normally corresponds with PVA's amorphous structure was visible in the XRD spectra of pure PVA nanofibers [39].

For polyether polyurethane characteristic diffraction peaks appeared at around 2θ=21°, and 2θ=23°. This peak is the characteristic of orthorhombic crystal structure of PU, which has been documented in previous studies [60].

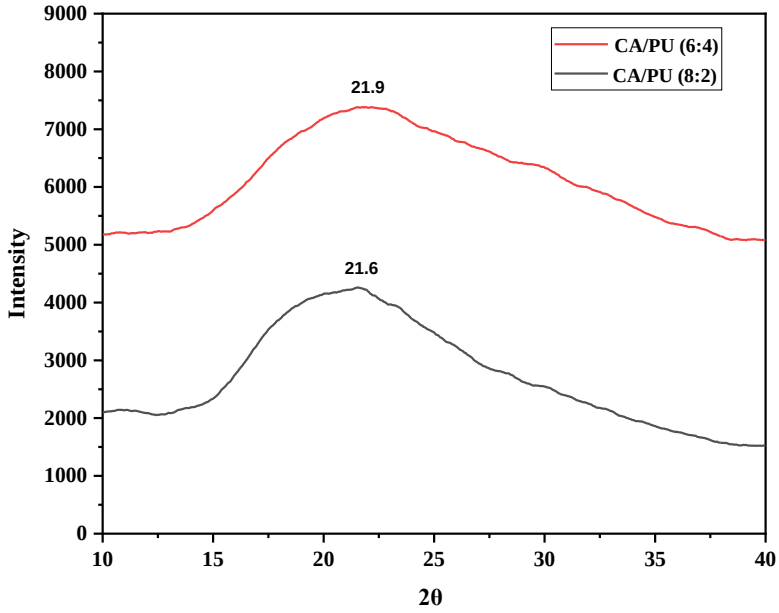

Figure 4.9 XRD spectra of CA/PU (6:4), CA/PU (8:2)

Figure 4.10 shows the peaks of CA/PU (6:4) and CA/PU (8:2) at 2θ = 21.9°, and 2θ= 21.6°. The peaks of CA/PU (6:4): PVA (CIP) and CA/PU (8:2): PVA (CIP) sheets can be seen at 2θ = 21.6°, and 2θ= 19.6, 21.9 ° respectively.

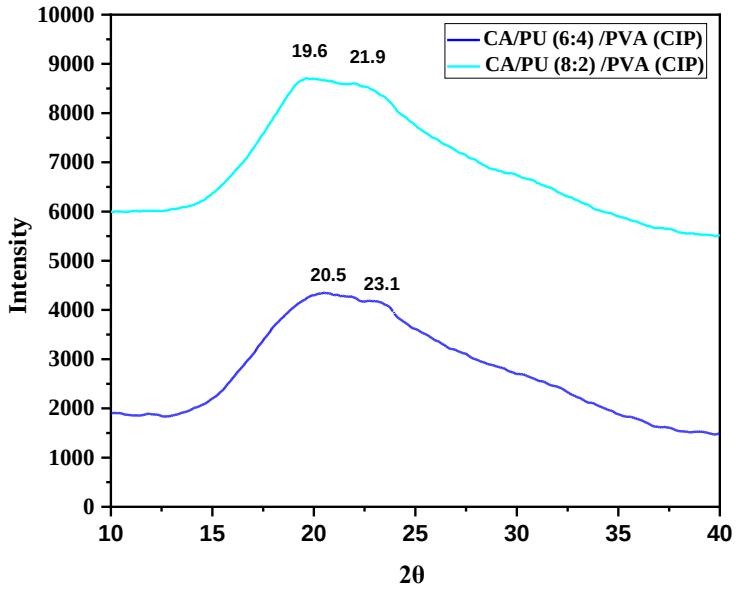

Figure 4.10 XRD spectra of CA/PU (6:4): PVA (CIP), CA/PU (8:2): PVA (CIP)

The XRD pattern of the blend of polyether polyurethane (PU) and cellulose acetate (CA) in a 8:2 ratio showed peak at 2θ value of 21.9°, as shown in Figure 4.1. The presence of a single peak at 21.9° suggests that the blend may have undergone some degree of miscibility or interaction between the two polymers such as formation of hydrogen bonding. The blend composition resulted in the suppression of some of the peaks. Overall, the observed XRD pattern suggests that the CA and PU in the blend have undergone some degree of interaction and have formed a new phase with a more amorphous structure. Previous studies have also reported similar results for blends of CA and PU, where the XRD patterns show a single peak at 20-22° due to the formation of a new amorphous phase or the suppression of individual peaks [61].

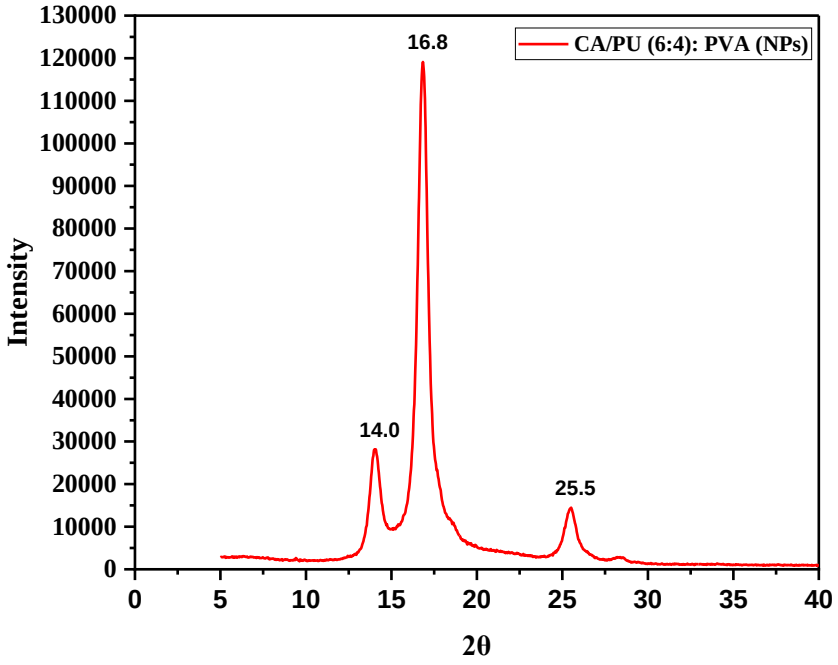

Figure 4.11 XRD analysis CA/PU (6:4): PVA (NPs)

To assess the crystallinity of the nanofibers, the XRD spectra of pure PVA, pure CA, pure PU, their blends with free ciprofloxacin and ciprofloxacin nanoparticles were analyzed. Figure 4.10 depicts the significant wide peak at 2θ = 19.4°, demonstrating the pure crystalline nature of PVA. Figure 3.9 shows the cipro characteristics peaks at 2θ =12.1°, 20.1°, 25.2°, 26.4°, 38.6°, 16.9°, and 19.0 pointing to the drug's regular crystal structure. The XRD pattern indicates that the PVA electrospun sheet's crystallinity was not significantly changed by the addition of ciprofloxacin. Similar results have been reported for PVA-based electrospun sheets loaded with other drugs (Zhang et al., 2015; Zhou et al., 2018). XRD analysis confirmed the crystal nature of PVA and the amorphous nature of ciprofloxacin in the PVA (CIP) electrospun sheet [62].

3.2.4 Thermogravimetric measurements (TGA)

TGA is a strategy used to study the thermal stability and decomposition behavior of a material. The sample is continuously heated, and its weight is measured as a function of either temperature or time. As the sample is heated, it undergoes various chemical and physical changes, such as phase transitions, degradation, and combustion. These changes result in a change in the weight of the sample, which is recorded by the TGA instrument. The data obtained from TGA can be used to determine various parameters such as onset temperature, peak temperature, rate of decomposition, and residual weight. TGA is a widely used technique in various fields such as materials science, polymer chemistry, and pharmaceuticals. It is particularly useful in the characterization of polymers, composites, and other organic materials.

TGA was utilized to examine the thermogravimetric analysis (TGA) of electrospun CA, PVA, PU, CA/PU (8:2), CA/PU: PVA (CIP), and CA/PU: PVA (NPs).

The thermal degrading behavior of CA electrospun fibers in graph (A) can be seen at 42°, between 278° and 530°. The PVA sheet (B) showed degradation at 41°, 225° and completed at 498°. There were two step degradation shown in PU graph (C) at 291°, 351° and 504°. In graph (D), the degradation points of CA/PU (8:2) can be noted at 46°, 255°,478° and 550°. For the CA/PU: PVA (CIP) in figure (4.3), it can be seen at 47°,260° and

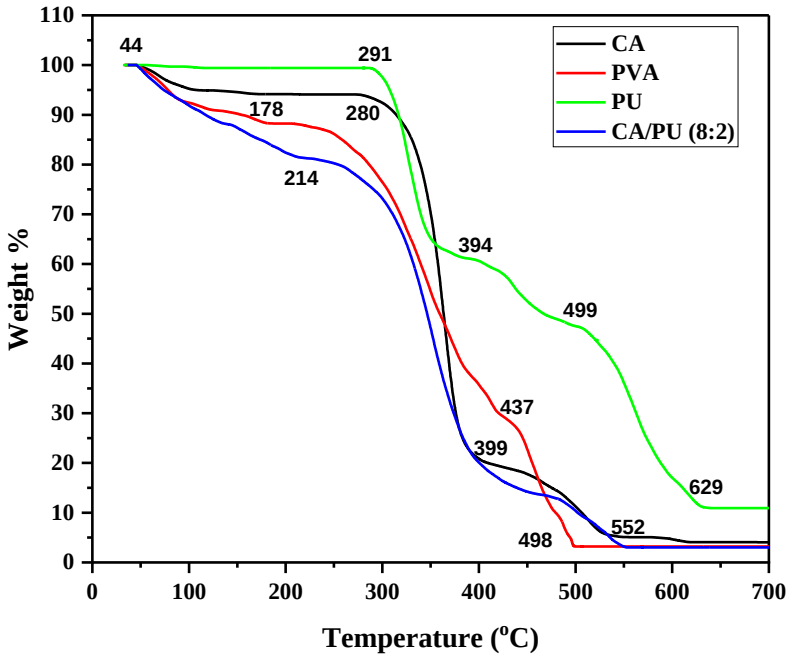

Figure 4.12 Thermogravimetric analysis of control sheets CA, PVA, PU and CA/PU (8:2)

According to TGA data, all materials were stable to heating at temperatures below 278 °C. The rapid weight loss at 300 C is caused by polysaccharide breakdown. According to Ahn et al. (2012), the breakdown temperature for ordinary cellulose is between 320 and 400 C [63]. Thermal breakdowns of the CA chains brought to the termination of the second stage. Following the second stage, the deteriorated products turned into ash, demonstrating the heat breakdown of the cellulose-based compounds. The thermal degrading behavior of CA electrospun fibers can be separated into three stages. At 44, the first stage was observed. The second stage, which is the thermal degradation stage of the polymer, was detected at around 278°C. At 405°C, the third step is related to polymer backbone cleavage. The greater part of the mass loss, which was attributable to CA degradation, occurred between 405°C and 530 °C, according to the weight loss curve of the original CA [64]. The TGA curve of PU showed a great weight loss in the range of 291-504°C due to the degradation of the soft segment and hard segment of the polymer The first weight loss occurred between 291°C and 351°C and was attributed to the

evaporation of residual moisture. The residue weight at 632°C was indicating the presence of inorganic content [58].

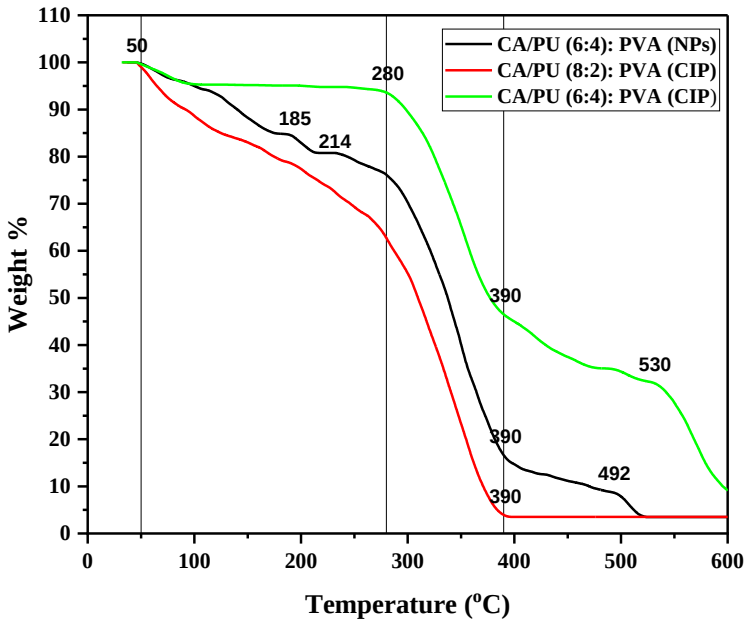

Figure 4.13 Thermogravimetric analysis of CA/PU (6:4): PVA (CIP), CA/PU (8:2): PVA (CIP), CA/PU (6:4): PVA (NPs).

In the TGA analysis of the CA/PU blend, it was observed that the weight loss occurred in three stages. The first stage showed a minor weight loss below 100 °C, which is attributed to the eradication of physically adsorbed moisture. The second stage, which occurred between 255-478 °C, showed a major weight loss due to the decomposition of both CA and PU. The third stage, which occurred above 478°C to 550°C, showed a residual weight loss showing the presence of inorganic content in the sample. Due to the presence of PVA in CA/PU: PVA (CIP) in figure (4.3), the temperature decreases to 47°C, at which point the moisture is evaporated and the whole sheet degrades between 260°C to 396°C [65].

3.2.5 Wettability / Contact Angle measurements

The wettability of a solid surface by a liquid is measured using the contact angle approach. It entails taking a measurement of the angle made by the liquid-solid interface and the tangent to the liquid surface where they meet the solid surface. Surface tension of the liquid, surface energy of the solid, and interfacial tension between the liquid and the solid all have an impact on the contact angle. Ineffective wetting of the solid surface is indicated by a high contact angle, whereas good wetting is indicated by a low contact angle. This technique is widely used in many fields such as material science, chemistry, and biology to study the surface properties of different materials, such as coatings, fibers, and membranes. It is also used to investigate surface modifications and their effects on the wettability of a surface.

In the present study, the contact angles of CA, PU, PVA, CA/PU (6:4), CA/PU (8:2) , CA/PU (6:4): PVA (CIP), CA/PU (8:2): PVA (CIP) and CA/PU (6:4): PVA (NPs) were measured using the sessile drop method. For the sheet CA/PU: PVA (CIP), both sides of the sheets were examined the CA/PU side as well as PVA (CIP) side.

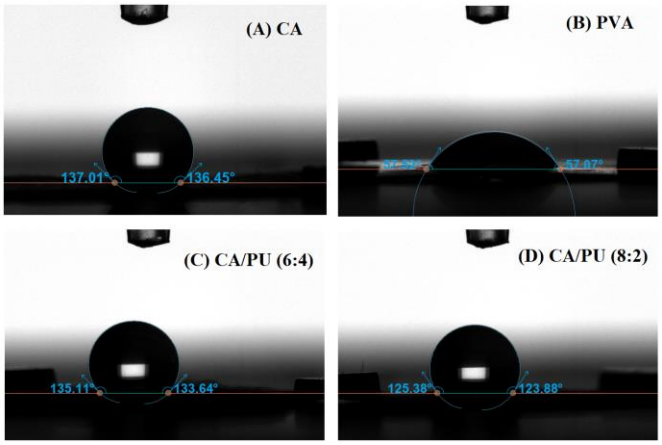

Figure 4.14 Contact angle measurements of (A) CA, (B) PVA, (C) CA/PU (6:4), (D) CA/PU (8:2)

The results showed CA with a contact angle of 128.13° ± 8.4. The composite sheet from CA/PU (6:4) side gave an angle of 131.42° ± 3.2 and the PVA (CIP) side showed 54.42° ± 3.3 that shows its hydrophilic character.

Table 4.1 Contact angle measurements of CA, PVA, CA/PU (6:4), CA/PU (8:2)

Compositions	Contact angle (°)	Surface free energy (mN/m)
CA	128.13 ± 8.4	11.51 ± 2.4
PVA	58.06 ± 3.1	48.52 ± 2.6
PU	141.88 ± 7.1	2.806 ± 1.9
CA/PU (6:4)	131.42 ± 3.2	4.95 ± 1.5
CA/PU (8:2)	116.66 ± 7.2	13.249 ± 3.9

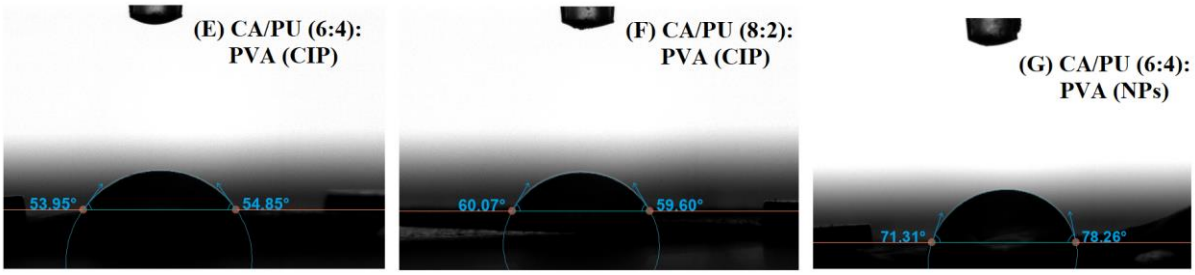

Figure 4.15 Contact angle and surface free energy of (E) CA/PU (6:4): PVA (CIP), (F) CA/PU (8:2): PVA (CIP), (G) CA/PU (6:4): PVA (NPs).

Cellulose acetate is a synthetic polymer that is widely used in the production of membranes, films, and fibers. It is known to have a hydrophobic nature because of the presence of acetyl groups on the polymer chain. The contact angle of cellulose acetate was measured to be 128.13° ± 8.4 [66]. indicating its hydrophobic nature. This means

that water tends to slide off the surface of cellulose acetate rather than wetting it. The hydrophobicity of the CA/PU blend electrospun sheets was found to be increased a little compared to the CA electrospun sheets due to the incorporation of PU [67]. The nanoparticles side of the composite sheets CA/PU (6:4): PVA (NPs) showed an angle of 60.35° ± 13.8 that showed the hydrophilic nature of the PVA which is suitable for the wound dressing materials.

Table 4.2 Contact angle and surface free energy of (E) CA/PU (6:4): PVA (CIP), (F) CA/PU (8:2): PVA (CIP), (G) CA/PU (6:4): PVA (NPs). Calculated in triplicates.

Compositions	Contact angle (°)	Surface free energy (mN/m)
CA/PU (6:4): PVA (CIP)	54.42 ± 3.3	48.716 ± 2.0
CA/PU (8:2): PVA (CIP)	66.69 ± 4.4	44.64 ± 2.2
CA/PU (6:4): PVA (NPs)	60.35 ± 13.8	44.428 ± 10.7

3.2.6 Density measurements

A pycnometer is a versatile laboratory instrument used to determine the density of liquids and solids. The ability of a pycnometer to provide accurate density measurements is one of its main advantages. The density can be calculated with high precision by knowing the precise volume of the pycnometer and measuring the mass of the substance it contains. The densities of the polymeric sheets of CA, PU, PVA, CA/PU (6:4), CA/PU (8:2), CA/PU (6:4): PVA (CIP), CA/PU (8:2): PVA (CIP), CA/PU (6:4): PVA (NPs) were measured and are given in the table (4.3) [68].

Table 4.3 Densities of the electrospun sheets

Compositions	Density (g/cc)
CA	0.0259 ± 0.024
PVA	0.0156 ± 0.002
PU	0.0163 ± 0.012
CA/PU (6:4)	0.0050 ± 0.004
CA/PU (8:2)	0.0623 ± 0.003
CA/PU (6:4): PVA (CIP)	0.0231 ± 0.016
CA/PU (8:2): PVA (CIP)	0.0862 ± 0.016
CA/PU (6:4): PVA (NPs)	0.0097 ± 0.013

3.2.7 Dynamic Mechanical Analysis (DMA)

Dynamic Mechanical Analysis (DMA) is a technique for determining the viscoelastic behaviour of a material, such as stiffness, damping, and the ability to store and dissipate energy. DMA involves applying a sinusoidal stress or strain input to a material and measuring the mechanical response.

The stress-strain curves for electrospun sheets are given in Figure 4.16. According to the results, CA nanofibres have a high mechanical strength, but CA/PU (8:2): PVA (CIP) composite nanofibers have a very high mechanical strength, which is higher than all other fibres.

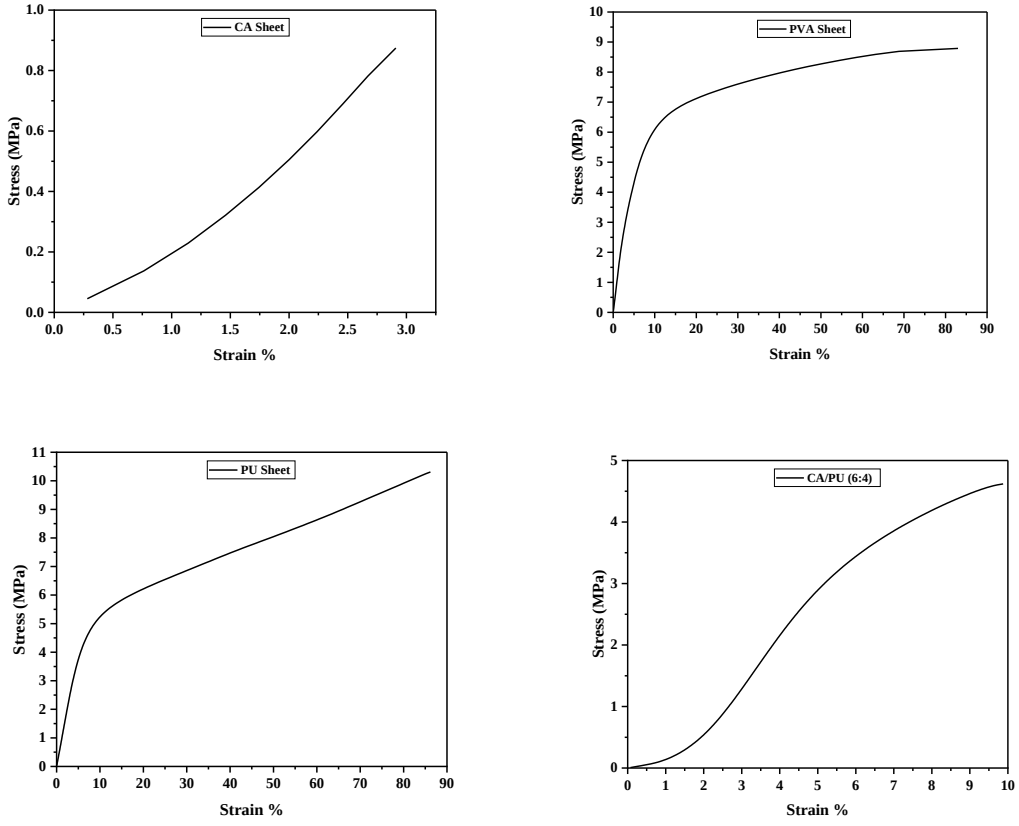

Figure 4.16 Stress-strain curves of CA, PVA, PU, CA/PU (6:4), Measured in triplicates.

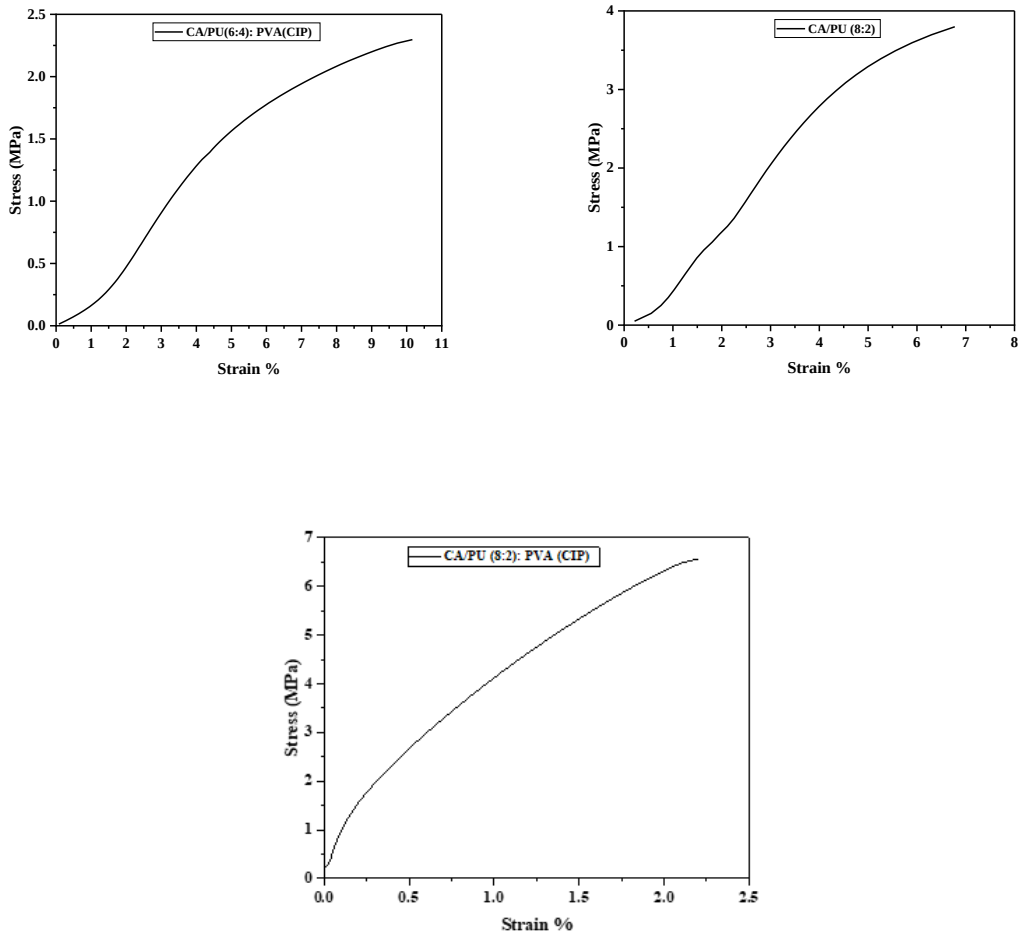

Figure 4.17 Stress-strain curves of CA/PU (8:2), CA/PU (6:4): PVA (CIP), CA/PU (8:2): PVA (CIP)

The measured density for all the electrospun sheets having the ciprofloxacin and the drug loaded nanoparticles indicates a low density that can be attributed to the presence of void spaces or pores within the material. The porosity having an inverse relation with the density tells us that lower the density, higher the porosity. The fabricated sheets are of a high porosity [69].

3.2.8 Antibacterial activity

Antibacterial activity refers to the ability of a substance or agent to inhibit the growth or kill bacteria. It is an important property of antimicrobial agents, including antibiotics, disinfectants, and other compounds used to combat bacterial infections [70].

The antibacterial activity of the sheets CA/PU (6:4): PVA(NPs), CA/PU (8:2): PVA (CIP), CA/PU (6:4), CA/PU (8:2) were performed against *E.coli* and *S.aureus.*

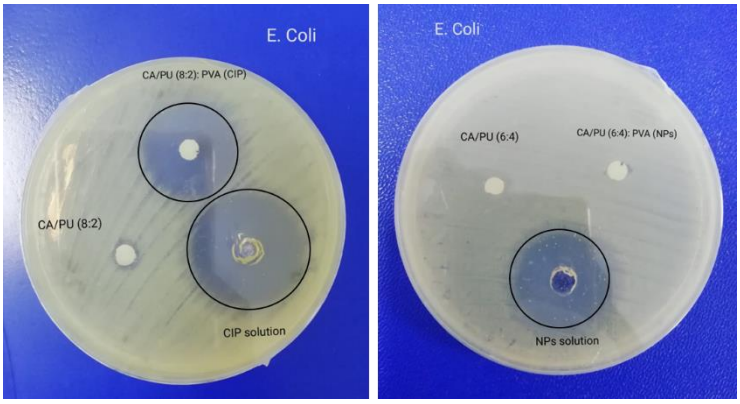

Figure 4.18 Antibacterial activity of CA/PU (6:4): PVA(NPs), CA/PU (8:2): PVA (CIP), CA/PU (6:4), CA/PU (8:2) as a negative control, CIP solution and NPs solution as a positive control against *E.coli*

Due of the prolonged release of the drug from the nanoparticles, the CA/PU (6:4): PVA (NPS) displayed no antibacterial action, whereas the CIP-loaded sheet CA/PU (8:2): PVA (CIP) demonstrated an inhibitory zone of 30 mm and 25mm against *E.coli* and *S.aureus.* The CIP solution and NPs solution as controls gave inhibition zone of 32 to 18 mm against both strains [71].

The zones by the sheets given are shown in the table (4.4).

Table 4.4 Zones of inhibition of CA/PU (6:4): PVA (CIP), CIP solution and NPs solution against *E.coli*

samples	Zones (mm)
CA/PU (8:2): PVA (CIP)	30 ± 0 mm
CIP solution	32.3 ± 2.6 mm
NPs solution	25 ± 4.1 mm

The sheets loaded with ciprofloxacin and the nanoparticles were checked against S.aureus as shown in the figure (4.19)

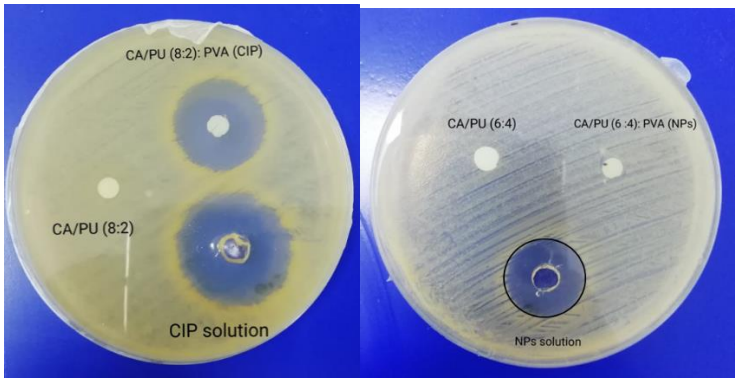

Figure 4.19 Antibacterial activity of CA/PU (6:4): PVA(NPs), CA/PU (8:2): PVA (CIP), CA/PU (6:4), CA/PU (8:2) as a negative control, CIP solution and NPs solution as a positive control against *S.aureus*

Table 4.5 Zones of inhibition of CA/PU (6:4): PVA (CIP), CIP solution and NPs solution against *S.aureus*

samples	Zones (mm)
CA/PU (8:2): PVA (CIP)	25± 0.5 mm
CIP solution	32 ± 2.8 mm
NPs solution	18 ± 2.1 mm

3.2.9 Drug release

After 7 days drug release, it was noted that the sheet with drug CA/PU (6:4): PVA (CIP) showed the 20% release of drug and the nanoparticles loaded sheet CA/PU (6:4): PVA (NPs) showed a sustained release of 5% as shown in figure (4.20).

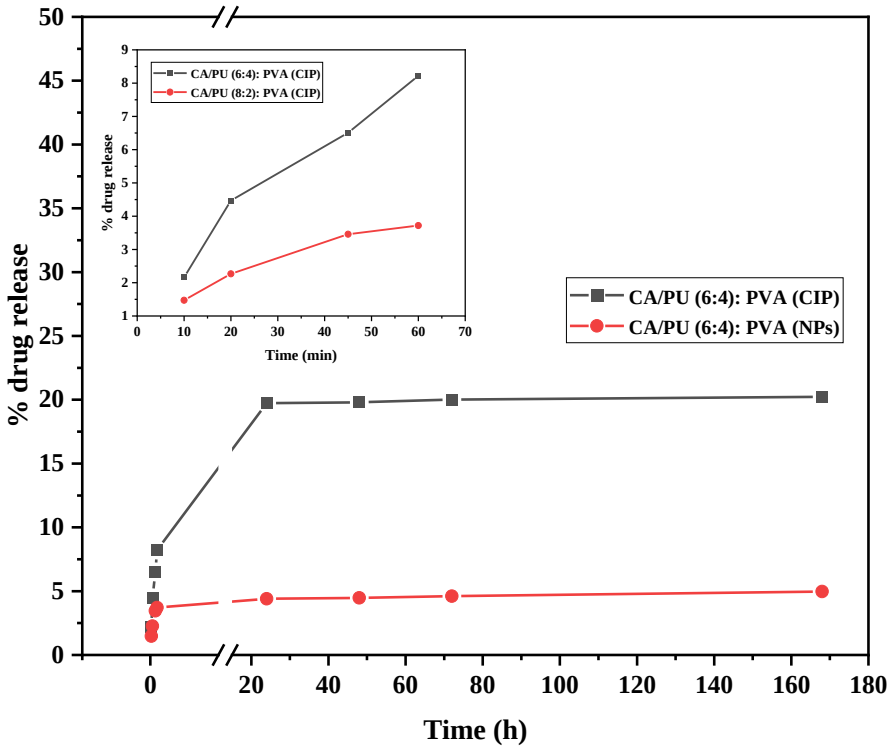

Figure 4.20 Drug release from CA/PU (6:4): PVA (CIP), CA/PU (6:4): PVA (NPs), CA/PU (8:2): PVA (CIP) at time intervals in minutes and hours. The experiment was performed in triplicates.

Drug release refers to the process by which a pharmaceutical drug is released from its dosage form or delivery system, such as tablets, capsules, patches, implants, or nanoparticles, and becomes available for absorption and distribution within the body [72]. The drug release study of the drug and nanoparticles loaded electrospun sheets was evaluated till 7 days and still going on till 21 days to see the total drug release behavior from both the composite sheets. The sheet CA/PU (6:4): PVA (CIP) show the 20 % release in 7 days and the sheet loaded with the nanoparticles showed a sustained release. [72]

Chapter 5

Conclusion

In conclusion, our study concentrated on the design and development of electrospun membranes containing novel nanoparticles for wound healing applications. We wanted to look into the characteristics and properties of these membranes using various characterization techniques like FESEM, FTIR, contact angle measurement, density measurements, antibacterial activity, and drug release in this study.

The smooth fibres of the electrospun sheets are required for drug and nanoparticle adhesion and delivery. The FTIR results revealed the formation of bilayer sheets as well as the incorporation of the drug and nanoparticles. The contact angle and density measurements revealed that the sheets are sufficiently hydrophilic and porous to be used as a wound healing material. The drug release revealed that the drug-incorporated sheets provided a slight burst release of the drug, whereas the nanoparticles-loaded sheets provided a sustained release of the drug. In terms of antibacterial activity, the drug-loaded membranes inhibited bacterial growth after 24 hours, indicating burst release, whereas the NPs-loaded sheet did not provide zones after 24 hours. The researchers gained important insights into the properties of electrospun membranes loaded with drugs and drug-loaded nanoparticles, which are critical for their effectiveness in wound healing applications.

References

1. Hannen, R., et al., *Chapter 15 - Skin tissue engineering and keratinocyte stem cell therapy*, in *Tissue Engineering (Third Edition)*, J. De Boer, et al., Editors. 2023, Academic Press. p. 491-532.
2. Pedde, R.D., et al., *Emerging Biofabrication Strategies for Engineering Complex Tissue Constructs.* Advanced Materials, 2017. **29**(19): p. 1606061.
3. Chogan, F., et al., *Skin Tissue Engineering Advances in Burns: A Brief Introduction to the Past, the Present, and the Future Potential.* Journal of Burn Care & Research, 2023. **44**(Supplement_1): p. S1-S4.
4. Jorgensen, A.M., et al., *Advances in Skin Tissue Engineering and Regenerative Medicine.* Journal of Burn Care & Research, 2023. **44**(Supplement_1): p. S33-S41.
5. Cai, R., et al., *Technological advances in three-dimensional skin tissue engineering.* 2023. **62**(1).
6. Wu, D.T., et al., *Viscoelastic Biomaterials for Tissue Regeneration.* Tissue Engineering Part C: Methods, 2022. **28**(7): p. 289-300.
7. Agrawal, R., et al., *A role of biomaterials in tissue engineering and drug encapsulation.* Proceedings of the Institution of Mechanical Engineers, Part E: Journal of Process Mechanical Engineering, 2023: p. 09544089221150740.
8. Yu, J.R., et al., *Current and Future Perspectives on Skin Tissue Engineering: Key Features of Biomedical Research, Translational Assessment, and Clinical Application.* Advanced Healthcare Materials, 2019. **8**(5): p. 1801471.
9. Rahmati, M., et al., *Biological responses to physicochemical properties of biomaterial surface.* Chemical Society Reviews, 2020. **49**(15): p. 5178-5224.
10. Su, J., et al. *Hydrogel Preparation Methods and Biomaterials for Wound Dressing*. Life, 2021. **11**, DOI: 10.3390/life11101016.
11. Kumar, M., et al., *A review on polysaccharides mediated electrospun nanofibers for diabetic wound healing: Their current status with regulatory perspective.* International Journal of Biological Macromolecules, 2023. **234**: p. 123696.

12. Wang, L., et al., *Influence of the mechanical properties of biomaterials on degradability, cell behaviors and signaling pathways: current progress and challenges.* Biomaterials Science, 2020. **8**(10): p. 2714-2733.
13. Uhljar, L.É. and R. Ambrus *Electrospinning of Potential Medical Devices (Wound Dressings, Tissue Engineering Scaffolds, Face Masks) and Their Regulatory Approach*. Pharmaceutics, 2023. **15**, DOI: 10.3390/pharmaceutics15020417.
14. Mello Zamudio, R., et al., *Obtaining a freeze-dried biomaterial for skin regeneration: Reinforcement of the microstructure through the use of crosslinkers and in vivo application.* Materials Chemistry and Physics, 2022. **290**: p. 126544.
15. Ahmed Ismail, K., et al., *Perspectives on composite films of chitosan-based natural products (Ginger, Curcumin, and Cinnamon) as biomaterials for wound dressing.* Arabian Journal of Chemistry, 2022. **15**(4): p. 103716.
16. Chouhan, D., et al., *Emerging and innovative approaches for wound healing and skin regeneration: Current status and advances.* Biomaterials, 2019. **216**: p. 119267.
17. Pourshahrestani, S., et al., *Polymeric Hydrogel Systems as Emerging Biomaterial Platforms to Enable Hemostasis and Wound Healing.* Advanced Healthcare Materials, 2020. **9**(20): p. 2000905.
18. Arida, I.A., et al., *Electrospun polymer-based nanofiber scaffolds for skin regeneration.* Journal of Drug Delivery Science and Technology, 2021. **64**: p. 102623.
19. Haider, A., S. Haider, and I.-K. Kang, *A comprehensive review summarizing the effect of electrospinning parameters and potential applications of nanofibers in biomedical and biotechnology.* Arabian Journal of Chemistry, 2018. **11**(8): p. 1165-1188.
20. Zaarour, B., L. Zhu, and X. Jin, *A Review on the Secondary Surface Morphology of Electrospun Nanofibers: Formation Mechanisms, Characterizations, and Applications.* ChemistrySelect, 2020. **5**(4): p. 1335-1348.
21. Miguel, S.P., et al., *An overview of electrospun membranes loaded with bioactive molecules for improving the wound healing process.* European Journal of Pharmaceutics and Biopharmaceutics, 2019. **139**: p. 1-22.

22. Ullah, S. and X. Chen, *Fabrication, applications and challenges of natural biomaterials in tissue engineering*. Applied Materials Today, 2020. **20**: p. 100656.
23. Liakos, I.L., et al. *Electrospun Fiber Pads of Cellulose Acetate and Essential Oils with Antimicrobial Activity*. Nanomaterials, 2017. **7**, DOI: 10.3390/nano7040084.
24. Teixeira, M.A., M.T.P. Amorim, and H.P. Felgueiras *Poly(Vinyl Alcohol)-Based Nanofibrous Electrospun Scaffolds for Tissue Engineering Applications*. Polymers, 2020. **12**, DOI: 10.3390/polym12010007.
25. Kirsner, R.S. and W.H. Eaglstein, *The Wound Healing Process.* Dermatologic Clinics, 1993. **11**(4): p. 629-640.
26. Tolker-Nielsen, T., *Biofilm Development*, in *Microbial Biofilms*. 2015. p. 51-66.
27. Abdel Khalek, M.A., et al., *Photoactive electrospun cellulose acetate/polyethylene oxide/methylene blue and trilayered cellulose acetate/polyethylene oxide/silk fibroin/ciprofloxacin nanofibers for chronic wound healing.* International Journal of Biological Macromolecules, 2021. **193**: p. 1752-1766.
28. Teixeira, M.A., et al., *Tiger 17 and pexiganan as antimicrobial and hemostatic boosters of cellulose acetate-containing poly(vinyl alcohol) electrospun mats for potential wound care purposes.* International Journal of Biological Macromolecules, 2022. **209**: p. 1526-1541.
29. Elsayed, R.E., T.M. Madkour, and R.A. Azzam, *Tailored-design of electrospun nanofiber cellulose acetate/poly(lactic acid) dressing mats loaded with a newly synthesized sulfonamide analog exhibiting superior wound healing.* International Journal of Biological Macromolecules, 2020. **164**: p. 1984-1999.
30. Vashisth, P., et al., *A novel gellan–PVA nanofibrous scaffold for skin tissue regeneration: Fabrication and characterization.* Carbohydrate Polymers, 2016. **136**: p. 851-859.
31. Adeli, H., M.T. Khorasani, and M. Parvazinia, *Wound dressing based on electrospun PVA/chitosan/starch nanofibrous mats: Fabrication, antibacterial and cytocompatibility evaluation and in vitro healing assay.* International Journal of Biological Macromolecules, 2019. **122**: p. 238-254.

32. Unnithan, A.R., et al., *Electrospun antibacterial polyurethane–cellulose acetate–zein composite mats for wound dressing.* Carbohydrate Polymers, 2014. **102**: p. 884-892.
33. Muñoz-Escobar, A., Á.d.J. Ruíz-Baltazar, and S.Y. Reyes-López, *Novel Route of Synthesis of PCL-CuONPs Composites With Antimicrobial Properties.* Dose-Response, 2019. **17**(3): p. 1559325819869502.
34. Unnithan, A.R., et al., *Wound-dressing materials with antibacterial activity from electrospun polyurethane–dextran nanofiber mats containing ciprofloxacin HCl.* Carbohydrate Polymers, 2012. **90**(4): p. 1786-1793.
35. Makvandi, P., et al., *Metal-Based Nanomaterials in Biomedical Applications: Antimicrobial Activity and Cytotoxicity Aspects.* Advanced Functional Materials, 2020. **30**(22): p. 1910021.
36. Pramanik, A., et al., *A novel study of antibacterial activity of copper iodide nanoparticle mediated by DNA and membrane damage.* Colloids Surf B Biointerfaces, 2012. **96**: p. 50-5.
37. Rodríguez, K., P. Gatenholm, and S. Renneckar, *Electrospinning cellulosic nanofibers for biomedical applications: structure and in vitro biocompatibility.* Cellulose, 2012. **19**(5): p. 1583-1598.
38. El-Alfy, E.A., et al., *Preparation of biocompatible chitosan nanoparticles loaded by tetracycline, gentamycin and ciprofloxacin as novel drug delivery system for improvement the antibacterial properties of cellulose based fabrics.* International Journal of Biological Macromolecules, 2020. **161**: p. 1247-1260.
39. Chen, Y., et al., *Electrospun thymol-loaded porous cellulose acetate fibers with potential biomedical applications.* Materials Science and Engineering: C, 2020. **109**: p. 110536.
40. Riaz, T., et al., *Synthesis and characterization of polyurethane-cellulose acetate blend membrane for chromium (VI) removal.* Carbohydrate Polymers, 2016. **153**: p. 582-591.
41. Noosak, C., et al., *Bioactive functional sericin/polyvinyl alcohol hydrogel: biomaterials for supporting orthopedic surgery in osteomyelitis.* Journal of Materials Science, 2023. **58**(12): p. 5477-5488.

42. Uhljar, L.É., et al. *In Vitro Drug Release, Permeability, and Structural Test of Ciprofloxacin-Loaded Nanofibers*. Pharmaceutics, 2021. **13**, DOI: 10.3390/pharmaceutics13040556.
43. Choipang, C., et al., *Hydrogel wound dressings loaded with PLGA/ciprofloxacin hydrochloride nanoparticles for use on pressure ulcers.* Journal of Drug Delivery Science and Technology, 2018. **47**: p. 106-114.
44. Esmaeili, E., et al., *The biomedical potential of cellulose acetate/polyurethane nanofibrous mats containing reduced graphene oxide/silver nanocomposites and curcumin: Antimicrobial performance and cutaneous wound healing.* International Journal of Biological Macromolecules, 2020. **152**: p. 418-427.
45. Esfahani, H., R. Jose, and S. Ramakrishna *Electrospun Ceramic Nanofiber Mats Today: Synthesis, Properties, and Applications*. Materials, 2017. **10**, DOI: 10.3390/ma10111238.
46. Ahmed, M., et al., *Collagen–PVA Films Plasticized with Choline Acetate Ionic Liquid for Sustained Drug Release: UV Shielding, Mechanical, Antioxidant, and Antibacterial Properties.* ACS Applied Bio Materials, 2023. **6**(2): p. 663-673.
47. Latiyan, S., T.S.S. Kumar, and M. Doble, *Fabrication and evaluation of agarose-curdlan blend derived multifunctional nanofibrous mats for diabetic wounds.* International Journal of Biological Macromolecules, 2023. **235**: p. 123904.
48. Ahmed, A., G. Getti, and J. Boateng, *Ciprofloxacin-loaded calcium alginate wafers prepared by freeze-drying technique for potential healing of chronic diabetic foot ulcers.* Drug Delivery and Translational Research, 2018. **8**(6): p. 1751-1768.
49. Budi, S., B. Suliasih, and I. Rahmawati, *Size-controlled chitosan nanoparticles prepared using ionotropic gelation.* ScienceAsia, 2020. **46**: p. 457–461.
50. Shafiei, M., H. Jafarizadeh-Malmiri, and M. Rezaei, *Biological activities of chitosan and prepared chitosan-tripolyphosphate nanoparticles using ionic gelation method against various pathogenic bacteria and fungi strains.* Biologia, 2019. **74**(11): p. 1561-1568.

51. Semwal, A., et al., *Macromolecular Chitosan/ Ciprofloxacin Pro-Drugs: Synthesis, Physico-chemical and Biological Assess-ment for Drug Delivery Systems.* Journal of Polymer Materials, 2012. **29**: p. 1-13.
52. Sayyar, Z. and H. Jafarizadeh Malmiri, *Photocatalytic and antibacterial activities study of prepared self-cleaning nanostructure surfaces using synthesized and coated ZnO nanoparticles with Curcumin nanodispersion.* 2019. **234**(5): p. 307-328.
53. Eskandari-Nojedehi, M., H. Jafarizadeh-Malmiri, and J. Rahbar-Shahrouzi, *Hydrothermal green synthesis of gold nanoparticles using mushroom (Agaricus bisporus) extract: physico-chemical characteristics and antifungal activity studies.* 2018. **7**(1): p. 38-47.
54. Pal, D.B., et al., *Synthesis and characterization of bio-composite nanofiber for controlled drug release.* Journal of Environmental Chemical Engineering, 2017. **5**(6): p. 5843-5849.
55. Atila, D., D. Keskin, and A. Tezcaner, *Cellulose acetate based 3-dimensional electrospun scaffolds for skin tissue engineering applications.* Carbohydrate Polymers, 2015. **133**: p. 251-261.
56. Mohammadi, A., M. Barikani, and M. Barmar, *Synthesis and investigation of thermal and mechanical properties of in situ prepared biocompatible Fe3O4/polyurethane elastomer nanocomposites.* Polymer Bulletin, 2015. **72**(2): p. 219-234.
57. Bernal-Ballén, A., I. Kuritka, and P. Saha, *Preparation and Characterization of a Bioartificial Polymeric Material: Bilayer of Cellulose Acetate-PVA.* International Journal of Polymer Science, 2016. **2016**: p. 3172545.
58. Choi, Y., et al., *Antibacterial ciprofloxacin HCl incorporated polyurethane composite nanofibers via electrospinning for biomedical applications.* Ceramics International, 2013. **39**(5): p. 4937-4944.
59. Majumder, S., A. Sharif, and M.E. Hoque, *Chapter 9 - Electrospun Cellulose Acetate Nanofiber: Characterization and Applications,* in *Advanced Processing, Properties, and Applications of Starch and Other Bio-Based Polymers*, F.M. Al-Oqla and S.M. Sapuan, Editors. 2020, Elsevier. p. 139-155.

60. Choi, S.-M., S. Lee, and E.-J. Shin *Synthesis and Characterization of Biopolyol-Based Waterborne Polyurethane Modified through Complexation with Chitosan*. Nanomaterials, 2022. **12**, DOI: 10.3390/nano12071143.
61. Piotrowska-Kirschling, A. and J. Brzeska *The Effect of Chitosan on the Chemical Structure, Morphology, and Selected Properties of Polyurethane/Chitosan Composites*. Polymers, 2020. **12**, DOI: 10.3390/polym12051205.
62. Kataria, K., et al., *In vivo wound healing performance of drug loaded electrospun composite nanofibers transdermal patch.* International Journal of Pharmaceutics, 2014. **469**(1): p. 102-110.
63. Kim, S.W., et al., *Fabrication and Characterization of Cellulose Acetate/Montmorillonite Composite Nanofibers by Electrospinning.* Journal of Nanomaterials, 2015. **2015**: p. 275230.
64. Elmaghraby, N.A., et al., *Electrospun composites nanofibers from cellulose acetate/carbon black as efficient adsorbents for heavy and light machine oil from aquatic environment.* Journal of the Iranian Chemical Society, 2022. **19**(7): p. 3013-3027.
65. Sivakumar, M., et al., *Preparation and performance of cellulose acetate–polyurethane blend membranes and their applications – II.* Journal of Membrane Science, 2000. **169**(2): p. 215-228.
66. Iqhrammullah, M., et al. *Characterization and Performance Evaluation of Cellulose Acetate–Polyurethane Film for Lead II Ion Removal*. Polymers, 2020. **12**, DOI: 10.3390/polym12061317.
67. Ayyar, M., et al., *Surface, thermal and hemocompatible properties of novel single stage electrospun nanocomposites comprising polyurethane blended with bio oil^{TM}*. Anais da Academia Brasileira de Ciências, 2017. **89**.
68. Lyu, Q., et al., *Moist-Induced Electricity Generation by Electrospun Cellulose Acetate Membranes with Optimized Porous Structures.* ACS Applied Materials & Interfaces, 2020. **12**(51): p. 57373-57381.

69. Cai, J., et al., *Well-aligned cellulose nanofiber-reinforced polyvinyl alcohol composite film: Mechanical and optical properties.* Carbohydrate Polymers, 2016. **140**: p. 238-245.
70. Aliagha, P., S. Amiri, and M. Ghiass, *Synthesis and characterization of nanofiber of gelatin, polyvinyl alcohol, and chitosan for wound dressing application.* The Journal of The Textile Institute, 2023: p. 1-10.
71. Homaeigohar, S. and A.R. Boccaccini, *Antibacterial biohybrid nanofibers for wound dressings.* Acta Biomaterialia, 2020. **107**: p. 25-49.
72. Kanimozhi, K., et al., *Development and Characterization of Sodium Alginate/Poly(vinyl alcohol) Blend Scaffold with Ciprofloxacin Loaded in Controlled Drug Delivery System.* J Nanosci Nanotechnol, 2019. **19**(5): p. 2493-2500.